https://doi.org/10.5194/bg-2023-128
Preprint. Discussion started: 9 August 2023
© Author(s) 2023. CC BY 4.0 License.

Biogeosciences Discussions
Open Access

Ecological evolution in northern Iberia (SW Europe) during the Late Pleistocene through isotopic analysis on ungulate teeth

Mónica Fernández-García[1(*)], Sarah Pederzani[2,3], Kate Britton[3], Lucía Agudo-Pérez[1], Andrea Cicero[1], Jeanne Marie Geiling[1], Joan Daura[4], Montserrat Sanz-Borrás[4], Ana B. Marín-Arroyo[1(*)]

1 Grupo de I+D+i EVOADAPTA (Evolución Humana y Adaptaciones durante la Prehistoria), Departamento de Ciencias Históricas, Universidad de Cantabria, 44. 39005 Santander, Spain

2 Department of Archaeology, University of Aberdeen, Aberdeen AB24 3UF, United Kingdom

3 Archaeological Micromorphology and Biomarkers Laboratory (AMBI Lab), Instituto Universitario de Bio-Orgánica "Antonio González", Universidad de La Laguna, 38206 San Cristóbal de La Laguna, Tenerife, Spain

4 Universitat de Barcelona, Grup de Recerca del Quaternari (GRQ-SERP), C/Montalegre 6-8, Barcelona 08001, Spain.

(*) Corresponding authors: anabelen.marin@unican.es, monica.fernandez.garcia.90@gmail.com

Abstract

During the Late Pleistocene, stadial and interstadial fluctuations affected vegetation, fauna, and human groups that were forced to cope with these pronounced climatic and environmental changes in time and space. These changes were especially abrupt during the Marine Isotopic Stage (MIS) 3. However, little is still known about the local and regional climatic conditions experienced by hominins in Europe. Here we reconstruct the climatic trends in northern Iberia considering the stable isotopic composition of ungulate skeletal tissues found in archaeological deposits dated between 80 to 15,000 cal BP. The carbon and oxygen isotopic composition preserved in the carbonate fraction of tooth enamel provides a reliable and high-resolution proxy of the food and water consumed by these animals, which is indirectly related to the local vegetation, environment, and climate, allowing us to estimate paleotemperatures and rainfall data. This study presents 44 bovine, equid, and cervid teeth from five archaeological sites in the Vasco-Cantabrian region (El Castillo, El Otero, Axlor, Labeko Koba, Aitzbitarte III) and one in the Mediterranean area (Canyars), where human evidence is attested from the Mousterian to the Magdalenian. The carbon isotope values reflect animals feeding on C3 plants with a mix-feeder diet mainly developed in open environments. However, carbon isotope value ranges point to differentiated ecological niches for equids and bovines, especially during the Aurignacian in the Vasco-Cantabrian region. Temperature estimations based on oxygen isotopic compositions and rainfall obtained from carbon isotopic compositions indicate colder and more arid conditions than nowadays from the Late Mousterian to the Aurignacian. The contemporary Mediterranean site shows slightly lower temperatures related to an arid period when animals mainly graze in open landscapes. In the Vasco-Cantabrian region, during the MIS2, the Gravettian data reflect a landscape opening, whereas the Magdalenian point to warmer conditions but still arid.

Keywords: Middle and Upper Palaeolithic; Neanderthal; Homo sapiens, palaeoecology; geochemistry

1. Introduction

Understanding the local and regional climatic evolution during the Late Pleistocene in southern Europe is crucial for assessing the potential impact of climate on the adaptation and decline of Neanderthals, as well as the subsequent expansion and resilience of Anatomically Modern Humans during the Upper Paleolithic. During the Late Pleistocene, the climatic records demonstrate stadial and interstadial continuous fluctuations during the Marine Isotope Stage 3 (MIS 3, ca. 60-27 ka) and MIS 2 (ca. 27-11 ka). Human groups had to face those episodes, which affected different vegetation and fauna depending on the region.

https://doi.org/10.5194/bg-2023-128
Preprint. Discussion started: 9 August 2023
© Author(s) 2023. CC BY 4.0 License.

Northern Iberia is a key study area due to the abundance of well-preserved archaeological caves and rock shelters where, in the last decade, an updated and multidisciplinary approach has been applied to disentangle how changing environmental conditions affected the subsistence dynamics of Middle and Upper Paleolithic hominins. Recent chronological, technological, and subsistence studies are revealing a more complex panorama than previously known.

The Vasco-Cantabrian region, located in northwestern Iberia, is subject to the influence of Atlantic climatic conditions and has been widely debated as a region that was significantly impacted by the glacial-interglacial oscillations during the MIS3 (Vidal-Cordasco et al., 2022). Modelling of traditional environmental proxies (small vertebrates and pollen) from archaeo-paleontological deposits show a progressive shift in the climatic conditions with decreasing temperatures and rainfall levels detected during the late Mousterian (Fernández-García et al., 2023). Ecological alterations have been observed in large mammals, such as niche partitioning between horses and cervids, a decrease in the available biomass for secondary consumers, and consequently decrease in herbivores carrying capacity (Jones et al., 2018; Vidal-Cordasco et al., 2022). Cold and arid conditions are maintained during the Aurignacian and the Gravettian until the onset of MIS2. Afterwards, during the Last Glacial Maximum (LGM, 23-19 ka), the global climatic deterioration associated with this glacial phase results in colder and more arid conditions in the region, with a predominance of open landscapes. However, this region still provided resources for human exploitation survival acting as a refugia area with more humid conditions in comparison to the Mediterranean area (Cascalheira et al., 2021; Garcia-Ibaibarriaga et al., 2019a; Lécuyer et al., 2021; Fernández-García et al., 2023; Fagoaga, 2014; Posth et al., 2023). By the end of the LGM, a climate amelioration and a moderate expansion of the deciduous forest are documented from the late Solutrean through the Magdalenian (Jones et al., 2021; Garcia-Ibaibarriaga et al., 2019a).

In contrast, northeastern Iberia is influenced by the Mediterranean climate. During MIS 3, this period has frequently been described as characterised by colder temperatures, higher rainfall compared to the present, and less pronounced climatic fluctuations when compared to the Vasco-Cantabrian region (López-García et al., 2014; Fernández-García et al., 2020; Vidal-Cordasco et al., 2022). Small-vertebrate communities and archaeobotanical evidence indicate relatively stable climatic conditions, but also the persistence of open forests during the Middle to Upper Paleolithic transition as in northwestern Iberia (Allué et al., 2018; Ochando et al., 2021). However, certain records indicate specific climatic excursions, such as increased aridity and landscape opening during Heinrich Events 4 and 5 (e.g., Álvarez-Lao et al., 2017; Daura et al., 2013; López-García et al., 2022; Rufí et al., 2018).

These multi-proxy studies have significantly expanded our understanding of the environment in Iberia. However, there is still limited availability of high-resolution proxies directly linked to human activity. In this study, we propose to investigate the ecology and environmental dynamics of past ungulates during the late Middle and Upper Paleolithic by measuring the carbon and oxygen isotopic composition ($\delta^{13}C$, $\delta^{18}O$) of bioapatite carbonates preserved in archaeological mammal teeth. Tooth enamel forms incrementally and does not biologically remodel, in contrast to other body tissues such as bone, which implies that the isotope values measured on them reflect the animal diet and water sources consumed during its mineralisation, around one to two years of animal life in our study species. The preserved carbon and oxygen isotope composition in the carbonate fraction of tooth enamel offers a high-resolution record of the dietary choices of the plants and water animals consume, which indirectly reflects the vegetation, environmental conditions, and climate.This allows us to estimate past temperatures, rainfall, and moisture levels on a sub-annual scale, returning isotopic information of the foraging areas where animals were feeding during tooth formation.

By analysing the stable isotopic composition of 44 ungulate teeth obtained from 15 archaeological levels associated with human occupation, including El Castillo, El Otero, Axlor, Labeko Koba, Aitzbitarte III in northwestern Iberia, and Terrasses de la Riera dels Canyars in northeastern Iberia, this study presents novel insights into local and regional environmental and climatic trends during the Late Pleistocene (Fig.1; Fig.2; Appendix A). Specifically, it focuses on the Middle to Upper Paleolithic transition in both areas and the post-

https://doi.org/10.5194/bg-2023-128
Preprint. Discussion started: 9 August 2023
© Author(s) 2023. CC BY 4.0 License.

LGM period in the Vasco-Cantabrian region. The main objectives of this work are: 1) to assess how regional environmental conditions, including changes in moisture and vegetation cover, but also temperatures and rainfall are recorded in tooth enamel stable isotopic composition; 2) to approach animal diet and their ecological niches; 3) to obtain quantitative temperature data to compare with available proxies; 4) to characterise seasonal patterns of animals found in the archaeological sites by identifying winter and summer fluctuations. The chronological resolution in the study areas for this period allows us to correlate regional paleoenvironmental changes with global records.

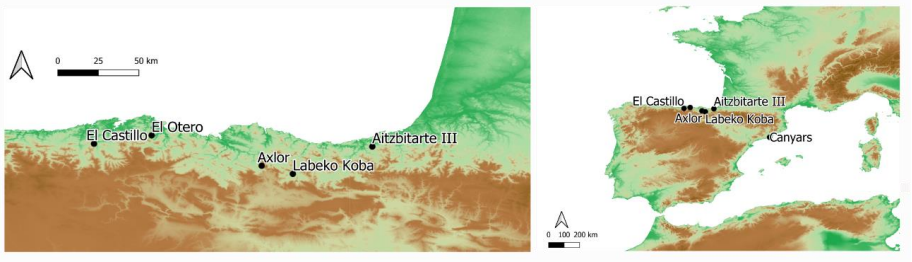

Figure 1. Location of the archaeological sites included in this work. From west to east, in the autonomous community of Cantabria, El Castillo, and El Otero; in the Basque Country, Axlor and Aitzbitarte III; in Catalonia, Canyars.

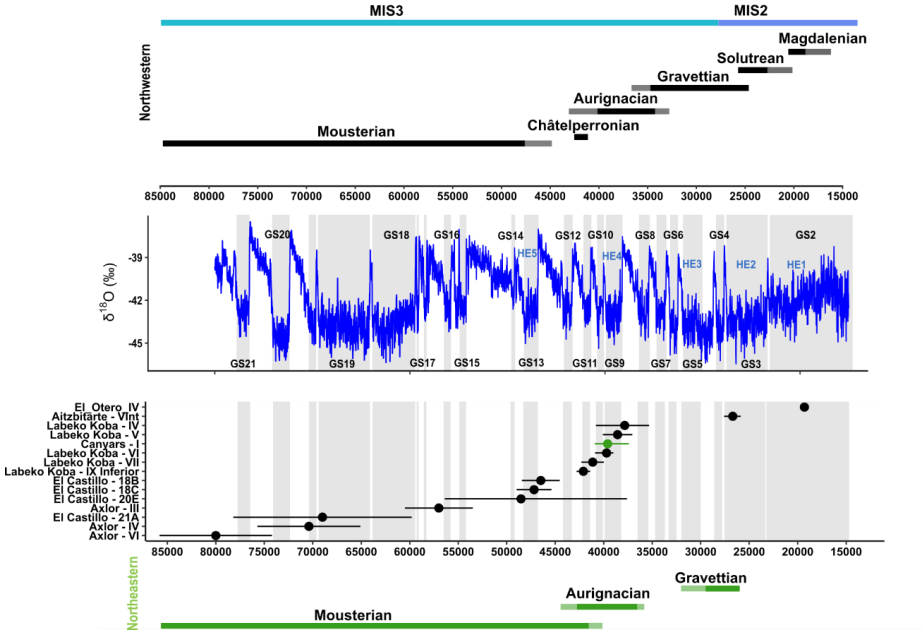

Figure 2. The temporal position of the archaeological levels included in the study is shown to the occurrence of different techno-complexes in both northwestern and northeastern Iberia, as well as the d^{18}O record from the NGRIP ice core (North Greenland Ice Core Project members, 2004; Rasmussen et al., 2014). Detailed chronological information is presented in Appendix B.

2. Archaeological sites and sampled material

This study selected a total of 44 ungulate teeth including 25 bovines (*Bos primigenius, Bison priscus, Bos/Bison* sp.), 14 equids (*Equus* sp. and *Equus ferus*), and 5 cervids (*Cervus elaphus*) found in five archaeological sites in the Vasco-Cantabrian region (El Castillo, El Otero, Axlor, Labeko Koba, Aitzbitarte

https://doi.org/10.5194/bg-2023-128
Preprint. Discussion started: 9 August 2023
© Author(s) 2023. CC BY 4.0 License.

III) and one in the Mediterranean area (Terrasses de la Riera dels Canyars, henceforth Canyars. These teeth were recovered from 15 archaeological levels attributed to the following technocomplexes: Mousterian (n=14), Transitional Aurignacian (n=10), Châtelperronian (n=2), Aurignacian (n=12), Gravettian (n=1) and Magdalenian (n=5) (Table 1 and 2; Appendix B). Archaeozoological studies of the archaeological sites are available (synthesis in Marín-Arroyo and Sanz-Royo, 2022; Daura et al., 2013) and most prove that faunal remains were accumulated by human acquisition during the different cultural phases. The isotopic results of equids from El Castillo were previously published by Jones et al. (2019) in combination with the bone collagen stable isotopes on ungulate prey capture at the site, as well as bioapatite phosphate analyses of bovines from Axlor (Pederzani et al., 2023).

3. Methods

3.1 Tooth sampling

All teeth included were sequentially sampled to reconstruct the complete $\delta^{18}O$ and $\delta^{13}C$ intratooth profiles based on enamel carbonate bioapatite. Intratooth sequential sampling was applied to the second and third molars and third and fourth premolars. Bovine and horse teeth sampled exceeded 3-4 cm of crown height to ensure that at least a one-year isotopic record of animal life was obtained (Hoppe et al., 2004; Britton et al., 2019). Samples were taken perpendicular to the growth axis on the tooth where the enamel was best preserved, avoiding, whenever possible taphonomic alterations such as cracks or postdepositional damages. Samples were performed in the labial face for the lower teeth and the lingual part for the upper ones. The outermost enamel surface was abraded to remove the superficial enamel, calculus, cementum, or concretions adhering to the surface to avoid contaminations. The sequential sampling consisted of straight strips (ca. 8 x 1.5 x 1 mm) covering the width of the selected lobe, approximately every 2-3 mm, from the crown to the Enamel-Root-Junction (ERJ). The sample depth covered around 75% of the enamel depth, and dentine inclusion was avoided. A low-revolution variable-speed manual drill was used, equipped with 1 mm diamond-coated drill bits of conical and cylindrical shape. About 10-15mg of enamel powder was collected in each subsample, generating 693 subsamples for IRMS measures (see complete intratooth profiles in Appendix C).

Site	Level - Cultural period	Bovines	Horses	Red deer	Teeth	Subsamples
Axlor	VI - Mousterian	2			2	32
	IV - Mousterian	1			1	12
	III - Mousterian	4			4	62
El Castillo	21 A - Mousterian	2	1		3	47
	20 E - Mousterian	2	2		4	56
	18C - Trans. Aurignacian	4			4	66
	18B - Trans. Aurignacian	3	2	1	6	93
Labeko Koba	IX - Châtelperronian		1	1	2	24
	VII - ProtoAurignacian	3			3	68
	VI - Aurignacian		1		1	16
	V - Aurignacian	1	1		2	39
	IV - Aurignacian		1		1	16
Canyars	I - Aurignacian	2	3		5	76
Aitzbitarte III	V - Gravettian	1			1	18
El Otero	IV - Magdalenian		2	3	5	68
TOTAL		**25**	**14**	**5**	**44**	**693**

Table 1. Number of teeth sampled by species, archaeological sites and cultural periods.

3.2 Sample treatment and stable isotope mass spectrometry

Several authors have debated the necessity of chemical pre-treatments to remove organic matter and secondary carbonates from bioapatite carbonates before stable isotopic analysis. Some chemical treatments can introduce secondary carbonates, increase carbonate content, and alter the original isotopic

https://doi.org/10.5194/bg-2023-128
Preprint. Discussion started: 9 August 2023
© Author(s) 2023. CC BY 4.0 License.

signal (Snoeck and Pellegrini, 2015; Pellegrini and Snoeck, 2016). The "side effects" of these pre-treatments can compromise the final isotopic signal measured. For this reason, in this work, most of the samples were not pretreated, except for the equid samples from Labeko Koba and Aitzbitarte III, and the cervids and equids from El Otero that were sampled and pretreated in the context of the initial project. Pretreatment followed was established by Balasse et al. (2002), where around 7 mg of powdered enamel was prepared and pretreated with 3% of sodium hypochlorite (NaOCl) at room temperature for 24 h (0.1 ml/mg sample), and thoroughly rinsed with deionised water, before a reaction with 0.1M acetic acid for 4 h (0.1 ml/mg sample) (equivalent protocol in Jones et al., 2019). Samples were then thoroughly rinsed, frozen, and freeze-dried. NaOCl is one of the most common agents used for pretreating carbonates and works as a base that removes organic matter by oxidation. Although it is considered one of the most efficient agents for removing organic matter, it can induce the absorption of exogenous carbonates, such as atmospheric CO_2 and secondary carbonates (Snoeck and Pellegrini, 2015; Pellegrini and Snoeck, 2016). It is argued that using acetic acid after NaOCl pretreatment can remove exogenous carbonates absorbed during NaOCl application. However, it is unclear if all newly introduced carbonates are finally released and which effect they produce on the original isotopic composition. While variations in pretreatment methods exist among samples in this study, the lack of a universally accepted protocol necessitates careful consideration of any potential isotopic effects resulting from these differences. These samples were analysed in the Godwin Laboratory (Department of Earth Sciences, University of Cambridge). Enamel powder samples were reacted with 100% orthophosphoric acid for 2h at 70°C in individual vessels in an automated Gasbench interfaced with a Thermo Finnigan MAT253 isotope ratio mass spectrometer. Results were reported in reference to the international standard VPDB and calibrated using the NBS-19 standard (limestone, $\delta^{13}C$ = +1.95‰ and $\delta^{18}O$ = -2.2‰; Coplen, 2011) for which the precision is better than 0.08‰ for $\delta^{13}C$ and 0.11‰ for $\delta^{18}O$.

For the non-pre-treated samples, carbon and oxygen stable isotopic ratios were measured using continuous flow-isotope ratio mass spectrometry, specifically a Europa Scientific 20-20 IRMS coupled to a chromatograph, at the Iso-Analytical laboratory in Cheshire, UK. The samples were weighed into clean exetainer tubes after being flushed with 99.995% helium. Phosphoric acid was then added to the samples, and they were allowed to react overnight to ensure the complete conversion of carbonate to CO_2, following the method outlined by Coplen et al. (1983). The reference materials used for VPDB calibration and quality control of the analysis included: IA-R022 (calcium carbonate, $\delta^{13}C$ = -28.63‰, $\delta^{18}O$ = -22.69‰), NBS-18 (carbonatite, $\delta^{13}C$ = -5.01‰, $\delta^{18}O$ = -23.2‰), IA-R066 (chalk, $\delta^{13}C$ = +2.33‰; $\delta^{18}O$ = -1.52). The accepted values of the in-house standards IA-R022 and IA-R066 were obtained by calibrating against IAEA international reference materials, NBS-18 and NBS-19, and NBS-18 and IAEA-CO-1 (Carrara marble, $\delta^{13}C$ = 2.5‰, and $\delta^{18}O$ = -2.4‰), respectively. Additionally, in-house standards long-term measured were used: ILC1 (calcite, $\delta^{13}C$ = 2.13, $\delta^{18}O$ = -3.99‰), and Y-02 (calcite, $\delta^{13}C$ = 1.48, $\delta^{18}O$ = -9.59‰). The analytical precision of quality control standard replicates was better than 0.09‰ for $\delta^{13}C$ and better than 0.12‰ for $\delta^{18}O$.

3.3 Carbon stable isotopic compositions as environmental tracers

To unravel animal diet and to compare the different species, in standardised terms, it is necessary to consider the fractionation factor (ε^*) between $\delta^{13}C$ obtained by the animal on its diet and $\delta^{13}C$ recorded on enamel carbonates (Bocherens, 2003; Cerling and Harris, 1999). The ε^* estimated for large ruminant mammals results in an offset of around 14.1‰ between diet and dental enamel, which is commonly applied generally to medium-sized herbivores. However, it is well-known that this offset varies between species, considering animals' different physiological parameters. Recently, a formal model to predict species-specific diet-consumer isotopic offsets has been proposed, which uses body mass (BM) and digestive physiology

https://doi.org/10.5194/bg-2023-128
Preprint. Discussion started: 9 August 2023
© Author(s) 2023. CC BY 4.0 License.

as the main factors that regulating the ε* (Tejada-Lara et al., 2018). This model proposes the following prediction equations for ruminant or foregut fermenters (Equation 1: Eq.1) and hindgut fermenters (Eq. 2):.

(Eq. 1) $\varepsilon^* = 2.34+0.05\ (BM)$ [r^2=0.78; p-value=0.008]

(Eq. 2) $\varepsilon^* = 2.42+0.032\ (BM)$ [r^2=0.74; p-value=0.003]

In this work, we compare species with different digestive physiology, ruminants for bovines and cervids, and non-ruminants for equids. The ε* value was adjusted to each animal to avoid bias from digestive physiology when comparing these species. The following fractionation factors have been used: 14.6‰ for *Bos taurus* (Passey et al., 2005), 13.7‰ for *Equus caballus* (Cerling and Harris, 1999), and 13.2‰ for *Cervus elaphus* (Merceron et al. (2021) following (Eq. 1) for ruminants with a mean body mass of 125 kg.

Carbon isotopic composition in body tissues is considered a combination of diet (understood as consumed food), environment openness (and associated exposure to light), and the amount of precipitation. Having the precipitation in mind, Lécuyer et al. (2021) proposed to estimate Mean Annual Precipitations (MAP) from $\delta^{13}C$ preserved in enamel carbonates, derived from diets based on C3 plants. After transforming $\delta^{13}C$ from enamel carbonate ($\delta^{13}C_{carb}$) to $\delta^{13}C$ of the diet ($\delta^{13}C_{diet}$) using the fractionation factors established above, this work suggested transforming this value to $\delta^{13}C$ from vegetation ($\delta^{13}C_{leaf}$). The MAP estimation is based on least square regression developed by Rey et al. (2013) and based on Kohn (2010) dataset (Eq.4), which requires first to estimate the $\delta^{13}C_{leaf}$ (Eq. 3). The $\delta^{13}C$ values of atmospheric CO_2 ($\delta^{13}C_{atm}$) are fixed in -7‰ (Lécuyer et al., 2021; Leuenberger et al., 1992; Schmitt et al., 2012).

(Eq.3) $\delta^{13}C_{leaf}\ (VPDB) = (\delta^{13}C_{atm} - \delta^{13}C_{diet}) / [1+(\delta^{13}C_{diet} / 1000]$

(Eq.4) $Log1(MAP+300) = 0.092(\pm0.004) \times \delta^{13}C_{leaf} + 1.148(\pm0.074)$

The Lécuyer et al. (2021) equation incorporates the consideration of the pCO_2 effect on $\delta^{13}C_{leaf}$ estimation, which is expected to result in an offset of +1‰ from current levels (considering that pCO_2 was 180 ppm during the LGM, which is lower than the 300ppm experienced during the post deglacial around 15 ka). If this correction was not applied MAP results will be underestimated by -150mm.

3.4 Oxygen stable isotope compositions as environmental tracers

Intratooth profiles are known to provide a time-averaged signal compared to input isotopic signal during enamel formation (Passey et al., 2005). This signal attenuation is caused both by time-averaging effects incurred through the extended nature of amelogenesis and tooth formation, and through the sampling strategy. During mineralisation, the maturation zone, which is time-averaged, often affects a large portion of the crown height and might affect the temporal resolution of the input signal of the sample taken. To obtain climatically informative seasonal information on the analysed teeth, the application of the inverse modelling method proposed by Passey et al. (2005) is, therefore, required. This method allows us to computationally estimate the time-averaging effects of sampling and tooth formation to obtain more accurately the original amplitude of the isotopic input signal, thus to summer and winter extremes (Appendix D). This method considers parameters based on the amelogenesis trends of each species and sampling geometry, which are critical for a meaningful interpretation of intratooth isotope profiles. To evaluate the data's reproducibility and precision, the model also estimates the error derived from the uncertainty of the sampling and the mass spectrometer measurements. This method was initially developed for continuously growing teeth, taking into account a constant growth rate within a linear maturation model, which a progressive time-average increment as sampling advances along the teeth profile. The species studied in this research exhibit non-linear tooth enamel formation, particularly in later-forming molars (Bendrey et al., 2015; Zazzo et al., 2012; Passey and Cerling, 2002; Kohn, 2004; Blumenthal et al., 2014). Although the aforementioned model is not

https://doi.org/10.5194/bg-2023-128
Preprint. Discussion started: 9 August 2023
© Author(s) 2023. CC BY 4.0 License.

ideal, as it does not account for non-linear enamel formation and certain growth parameters for the species included are unknown, it is the best estimation based on the current state of the field and remains widely used (Pederzani et al., 2023, 2021a, b).

Stable oxygen isotopes from meteoric water (mainly derived from rainfall) have a strong relationship with mean air temperatures in mid to high latitudes (Rozanski et al., 1992; Dansgaard, 1964) on a regional-to-local scale. Obligate drinkers, such as bovines and horses, acquire this water and record its isotopic composition in their teeth and bones with a fixed, but species-specific offset (Pederzani and Britton, 2019). Considering this two-step relationship, past climatic conditions can be estimated. However, most of the temperature reconstructions based on $\delta^{18}O$ have considered the $\delta^{18}O$ from the phosphate fraction of bioapatite enamel to build linear correlations between tooth enamel and drinking water $\delta^{18}O$ and obtain climatic information. For this reason, the $\delta^{18}O$ from carbonates values obtained in this work ($\delta^{18}O_{carb}$) were converted into $\delta^{18}O$ from phosphates ($\delta^{18}O_{phos}$). To do so, first, to express in VSMOW notation, the $\delta^{18}O$ was corrected using the following correlation (Coplen et al., 1983; Brand et al., 2014):

(Eq.5) $\delta^{18}O_{carb}$ (VSMOW)= 1.0309 x $\delta^{18}O_{carb}$ (VPDB) + 30.91

Second, considering the relationship existent in tooth enamel between the carbonate and phosphate fraction (Iacumin et al., 1996; Pellegrini et al., 2011), from a compilation of the existent bibliography of modern animals measurements (Trayler and Kohn, 2017; Pellegrini et al., 2011; Bryant et al., 1996), Pederzani et al. (2023) proposed the following correlation:

(Eq.6) $\delta^{18}O_{phos}$ (VSMOW) = 0.941 x $\delta^{18}O_{carb}$ (VSMOW) - 7.16

Once the isotopic information is expressed in $\delta^{18}O_{phos}$ (VSMOW), we can estimate the $\delta^{18}O$ on meteoric waters ($\delta^{18}O_{mw}$). It is known that different physiological factors will condition how oxygen isotope composition is fixed in each mammalian group. Thus, usually, the correlations are species-specific and developed considering the particular physiology of each animal group. The correlation employed by this work relies on recent data compilations (Pederzani et al., 2021b, 2023). In the case of horses (Eq. 7), it has been considered the data combination of Blumenthal et al. (2019); Chillón et al. (1994); Bryant et al., 1994; Delgado Huertas et al., 1995), whereas for bovines (Eq.8) the data from D'Angela and Longinelli (1990) and Hoppe (2006) have been put together in Eq. 4. To estimate $\delta^{18}O_{mw}$ from red deer remains, we selected D'Angela and Longinelli (1990) correlation (Eq. 9):

(Eq.7) $\delta^{18}O_{mw}$ (VSMOW)= ($\delta^{18}O_{phos}$ (VSMOW) - 22.14) / 0.87

(Eq.8) $\delta^{18}O_{mw}$ (VSMOW)= ($\delta^{18}O_{phos}$ (VSMOW) - 22.13) / 0.85

(Eq.9) $\delta^{18}O_{mw}$ (VSMOW)= ($\delta^{18}O_{phos}$ (VSMOW) - 24.39) / 0.91

Finally, the mean annual temperatures (MAT) were calculated from $\delta^{18}O_{mw}$, considering the linear regression model relating $\delta^{18}O_{mw}$ and air temperatures from Iberia proposed by Fernández-García et al. (2019). This correlation is based on monthly climatic records (monthly mean $\delta^{18}O_{mw}$ and monthly mean air temperatures) from all Iberian stations from the Global Network of Isotopes in Precipitation, operated by the International Atomic Energy Association and the World Meteorological Organization (IAEA/ WMO, 2018).

(Eq. 10) MAT (°C) = 2.38(± 0.10) × $\delta^{18}O_{mw}$ + 28.19(± 0.58)
[r^2= 0.65; n=304; p-value >0.0001]

Following Pederzani et al. (2021b, 2021a), MAT was deduced from the $\delta^{18}O$ mean value between summer and winter in each tooth before modeling to reduce associated error and maximise number of usable data records. Summer and winter estimations were extracted from the obtained $\delta^{18}O$ values after inverse modeling application, to identify seasonal variation. Due to the uncertainties incurred from converting stable

https://doi.org/10.5194/bg-2023-128
Preprint. Discussion started: 9 August 2023
© Author(s) 2023. CC BY 4.0 License.

isotope measurements to palaeotemperature, the final estimations in this work should be considered exploratory and as a method of standardisation to make results comparable with different sites, data from different species, and other non-isotopic palaeoclimatic records. In these estimations, the associated error from converting $\delta^{18}O_{phos}$ to MAT is enlarged by the uncertainty derived from the transformation of $\delta^{18}O_{carb}$ (VPDB) to $\delta^{18}O_{phos}$ (VSMOW) (see Pryor et al., 2014; Skrzypek et al., 2016 for further discussion).

3.4 Present-day isotopic and climatic data

Present-day climatic conditions surrounding each site have been considered, allowing an inter-site comparison, essential for our study but also a regional to a global perspective. Considering current MATs and MAPs, estimated climatic data is expressed in relative terms as MAT and MAP anomalies. Present-day summer and winter temperatures were also considered. Present-day temperatures and precipitation values were obtained from the WorldClim Dataset v2 (Fick and Hijmans, 2017) (Appendix B). This dataset includes the average of bioclimatic variables between 1970-2000 in a set of raster files with a spatial resolution every 2.5 minutes. The exact location of the selected archeo-palaeontological sites was used, using geographical coordinates in the projection on modern climatic maps with QGIS software.

Present-day δ^{18}Omw values from the analysed sites' areas were obtained using the Online Isotopes in Precipitation Calculator (OIPC Version 3.1 (4/2017); Bowen, 2022) based on datasets collected by the Global Network for Isotopes in Precipitation from the IAEA/WMO (Appendix B).

Site	Level	Culture	Species	Tooth type	Code	n	δ13Ccarb VPDB (‰)	min	max	SD	Range	δ18Ocarb VPDB (‰)	min	max	SD	Range
Axlor	III	Mousterian	*Bos/Bison* sp.	LRM3	AXL59	14	-8.9	-9.6	-8.2	1.4	0.4	-6.0	-7.3	-5.2	0.7	2.1
Axlor	III	Mousterian	*Bos/Bison* sp.	LRM2	AXL60	18	-9.7	-10.0	-8.9	1.1	0.3	-5.7	-6.8	-4.6	0.7	2.2
Axlor	III	Mousterian	*Bos/Bison* sp.	LRM3	AXL65	13	-8.9	-9.3	-8.1	1.2	0.4	-6.0	-7.2	-4.6	0.8	2.6
Axlor	III	Mousterian	*Bos/Bison* sp.	LRM2	AXL66	16	-8.9	-9.8	-8.3	1.5	0.5	-4.8	-6.1	-3.8	0.7	2.3
Axlor	IV	Mousterian	*Bos/Bison* sp.	LRM2	AXL70	12	-9.1	-9.4	-8.6	0.7	0.3	-5.3	-7.3	-3.9	1.2	3.4
Axlor	VI	Mousterian	*Bos/Bison* sp.	LLM3	AXL77	14	-9.7	-10.2	-9.2	1.0	0.4	-6.2	-7.9	-5.0	0.9	2.9
Axlor	VI	Mousterian	*Bos/Bison* sp.	LLM3	AXL86	18	-9.9	-10.2	-9.3	0.9	0.3	-5.4	-6.5	-3.8	0.7	2.6
El Castillo	20E	Mousterian	*Equus* sp.	LRP3/LRP4	CAS60	14	-11.9	-12.5	-11.5	1.0	0.3	-3.3	-4.1	-2.4	0.4	1.6
El Castillo	20E	Mousterian	*Equus* sp.	LRP3/LRP4	CAS61	14	-12.2	-12.4	-12.1	0.3	0.1	-4.9	-5.8	-4.3	0.4	1.5
El Castillo	20E	Mousterian	*Bos/Bison* sp.	LLM2	CAS139	16	-11.6	-12.2	-11.2	0.9	0.3	-5.6	-6.3	-4.9	0.5	1.4
El Castillo	20E	Mousterian	*Bos/Bison* sp.	LLM2	CAS140	12	-11.5	-11.9	-11.1	0.8	0.3	-5.5	-6.3	-4.6	0.6	1.7
El Castillo	21A	Mousterian	*Bos/Bison* sp.	LLM3	CAS141	15	-11.2	-11.5	-10.9	0.6	0.2	-5.4	-6.5	-4.3	0.6	2.2
El Castillo	21A	Mousterian	*Bison priscus*	LLM3	CAS142	15	-11.2	-11.7	-10.9	0.7	0.2	-5.0	-5.7	-4.4	0.4	1.3
El Castillo	21A	Mousterian	*Equus* sp.	LLM3	CAS143	17	-12.6	-12.9	-12.5	0.4	0.1	-6.2	-7.2	-5.4	0.5	1.8
El Castillo	18B	Transitional Aurignacian	*Bos/Bison* sp.	ULM2	CAS132	13	-11.3	-11.5	-10.9	0.6	0.2	-6.2	-7.4	-4.9	0.7	2.6
El Castillo	18B	Transitional Aurignacian	*Bos/Bison* sp.	ULM2	CAS133	18	-10.9	-11.6	-10.5	1.1	0.3	-5.4	-6.5	-4.2	0.7	2.2
El Castillo	18B	Transitional Aurignacian	*Bos/Bison* sp.	ULM2	CAS134	18	-12.4	-12.8	-11.6	1.2	0.3	-5.4	-6.3	-4.5	0.5	1.8
El Castillo	18C	Transitional Aurignacian	*Bos/Bison* sp.	LLM3	CAS135	17	-11.3	-11.5	-11.0	0.5	0.2	-6.1	-6.6	-5.5	0.3	1.1
El Castillo	18C	Transitional Aurignacian	*Bos/Bison* sp.	LLM3	CAS136	17	-12.0	-12.5	-11.7	0.9	0.2	-5.8	-6.7	-5.0	0.6	1.7
El Castillo	18C	Transitional Aurignacian	*Bos/Bison* sp.	LLM3	CAS137	14	-10.2	-10.6	-9.9	0.7	0.2	-5.8	-6.5	-4.1	0.7	2.4
El Castillo	18C	Transitional Aurignacian	*Bos/Bison* sp.	LLM3	CAS138	18	-11.6	-11.8	-11.4	0.4	0.1	-5.3	-5.9	-4.8	0.3	1.2
El Castillo	18B	Transitional Aurignacian	*Cervus elaphus*	ULM2+ULM3	CAS8	11	-13.0	-14.9	-12.1	2.8	1.0	-6.8	-10.4	-4.1	2.1	6.3
El Castillo	18B	Transitional Aurignacian	*Equus* sp.	ULP3/ULP4	CAS58	19	-11.7	-11.8	-11.5	0.3	0.1	-6.6	-7.5	-5.6	0.5	1.8
El Castillo	18B	Transitional Aurignacian	*Equus* sp.	LLP3/LLP3	CAS59	14	-11.5	-11.7	-11.0	0.7	0.2	-4.0	-4.7	-3.5	0.4	1.2
Labeko Koba	IX inf	Chatelperronian	*Equus* sp.	URM3	LAB38	17	-12.0	-12.2	-11.9	0.3	0.1	-6.6	-7.7	-5.9	0.5	1.9
Labeko Koba	IX inf	Chatelperronian	*Cervus elaphus*	LLM2	LAB02	7	-12.3	-12.4	-12.1	0.3	0.1	-4.7	-6.0	-3.7	1.0	2.3
Labeko Koba	VI	Aurignacian	*Equus* sp.	URM2	LAB20	16	-12.0	-12.2	-11.8	0.4	0.1	-5.3	-6.1	-4.4	0.6	1.7
Labeko Koba	V	Aurignacian	*Equus* sp.	LRM3	LAB42	17	-11.9	-12.3	-11.5	0.2	0.7	-5.7	-6.6	-5.0	0.5	1.6
Labeko Koba	IV	Aurignacian	*Equus* sp.	LRM2	LAB36	17	-11.6	-11.8	-11.3	0.6	0.2	-5.9	-6.2	-5.5	0.2	0.7
Canyars	I	Aurignacian	*Equus* sp.	URM3	CAN01	12	-10.0	-10.4	-9.5	0.9	0.3	-4.8	-5.3	-4.3	0.3	1.1
Canyars	I	Aurignacian	*Equus ferus*	URM3	CAN02	17	-10.5	-10.7	-10.3	0.4	0.1	-4.4	-5.0	-3.6	0.5	1.4
Canyars	I	Aurignacian	*Equus ferus*	URP3/URP4	CAN03	17	-10.7	-11.2	-10.4	0.8	0.2	-4.8	-5.3	-4.0	0.4	1.4
Labeko Koba	VII	Aurignacian	*Bos primigenius*	LRM3	LAB53	23	-9.5	-10.1	-8.7	1.4	0.3	-5.7	-7.0	-4.2	0.9	2.8
Labeko Koba	VII	Aurignacian	*Bos primigenius*	LRM3	LAB55	23	-10.4	-11.5	-9.8	1.6	0.3	-5.1	-7.0	-2.7	1.2	4.3
Labeko Koba	VII	Aurignacian	*Bos/Bison* sp.	LRM3	LAB62	21	-9.7	-10.2	-9.1	1.2	0.3	-7.2	-8.1	-6.2	0.6	2.0
Labeko Koba	V	Aurignacian	*Bos primigenius*	LRM3	LAB69	21	-9.3	-10.3	-7.3	3.0	0.9	-7.2	-8.8	-5.5	0.9	3.3
Canyars	I	Aurignacian	*Bos primigenius*	ULM3	CAN04	14	-9.3	-9.8	-8.7	1.1	0.3	-3.6	-4.2	-2.6	0.5	1.6
Canyars	I	Aurignacian	Bos primigenius	ULM3	CAN05	14	-9.0	-9.5	-8.5	0.9	0.3	-5.5	-6.2	-5.0	0.4	1.2
Aitzbitarte III	V (int)	Gravettian	*Bos/Bison* sp.	LLM3	AITI10	17	-9.2	-9.6	-8.7	0.9	0.3	-5.5	-6.5	-4.3	0.5	2.2
El Otero	IV	Magdalenian	*Cervus elaphus*	LLM2+LLM3	OTE1	11	-11.4	-11.6	-11.2	0.4	0.1	-4.4	-5.8	-2.9	1.0	2.9
El Otero	IV	Magdalenian	*Cervus elaphus*	LLM2+LLM3	OTE5	10	-11.3	-11.5	-11.0	0.5	0.2	-5.1	-5.7	-3.8	0.6	1.9
El Otero	IV	Magdalenian	*Cervus elaphus*	LLM2+LLM3	OTE6	14	-11.4	-11.8	-10.6	1.2	0.3	-4.6	-5.4	-4.0	0.4	1.4
El Otero	IV	Magdalenian	*Equus* sp.	LLP3/LLP4	OTE11	17	-11.6	-11.8	-11.4	0.5	0.1	-5.0	-6.3	-3.9	0.7	2.4
El Otero	IV	Magdalenian	*Equus* sp.	LLP3/LLP4	OTE12	16	-11.3	-11.5	-10.9	0.6	0.1	-3.9	-4.9	-3.3	0.6	1.6

Table 2. Mean, maximum value (Max), minimum value (Min), and standard deviation (SD) of $\delta^{13}C$ and $\delta^{18}O$ values per archaeological site and level organised by cultural periods. n= number of intratooth subsamples measured. In tooth type: position (U, upper; L, lower); laterality (R, right; L, left); tooth (M, molar; P, premolar).

https://doi.org/10.5194/bg-2023-128
Preprint. Discussion started: 9 August 2023
© Author(s) 2023. CC BY 4.0 License.

4. Results

In northwestern Iberia, specifically in the Vasco-Cantabrian region, the mean $\delta^{13}C_{carb}$ values range from -8.9‰ to -13‰, with a mean value of -11‰ (SD = 1.2‰) (Table 2; Table 3). Considering species' different fractionation factors, the $\delta^{13}C_{carb}$ were transformed in $\delta^{13}C_{diet}$, resulting in mean values that extend from -23.5‰ to -27‰ (Fig. 4). It must be considered that average values may reflect slightly different periods or be affected by seasonal bias because different teeth encompass different periods, but it has been verified in our teeth that the variations are limited when the seasonal information of the sequential sampling is incorporated (±0.2; Appendix B). The carbon isotopic composition varies between species. The bovines have generally higher mean $\delta^{13}C_{carb}$ (from -8.9‰ to -12.4‰) than the horses (from -11.3‰ to -12.6‰), whereas the red deer samples fall within the horses' range (from -11.3‰ to -13‰). Average values of $\delta^{18}O_{carb}$ in all Vasco-Cantabrian individuals extend between -3.3‰ and -7.2‰ (mean = -5.5‰; SD = 0.8‰). When transformed to $\delta^{18}O$ expected from meteoric waters ($\delta^{18}O_{mw}$), with species-adapted correlations, the $\delta^{18}O_{mw}$ values range from -3.9‰ to -9.9‰. Less clear patterns in $\delta^{18}O_{carb}$ are observed between bovines and horses, with mean values of -5.7‰ and -5.2‰, respectively. In the Mediterranean area, the site of Canyars, both species have relatively high $\delta^{18}O_{carb}$ values that fall inside the range of variation observed in the Cantabria region, between -3.6‰ and -5.5‰ in bovines and between -4.4‰ and -4.8‰ in case of horses.

	Vasco-Cantabrian region (NW Iberia)				Mediterranean region (NE Iberia)			
	δ^{13}Ccarb VPDB (‰)	δ^{13}Cdiet VPDB (‰)	δ^{18}Ocarb VPDB (‰)	d18Omw VSMOW (‰)	δ^{13}Ccarb VPDB (‰)	δ^{13}Cdiet VPDB (‰)	δ^{18}Ocarb VPDB (‰)	d18Omw VSMOW (‰)
Mean	-11.0	-25.1	-5.5	-6.7	-9.9	-24.0	-4.6	-5.4
Max	-8.9	-23.5	-3.3	-3.9	-9.0	-23.6	-3.6	-4.3
Min	-13.0	-27.0	-7.2	-9.9	-10.7	-24.4	-5.5	-6.5
Range	4.1	3.5	3.9	6.0	1.7	0.8	1.9	2.2
SD	1.2	0.9	0.8	1.1	0.8	0.3	0.7	0.8
Mean	-10.4	-25.0	-5.7	-6.8	-9.1	-23.7	-4.5	-5.4
Max	-8.9	-23.5	-4.8	-5.7	-9.0	-23.6	-3.6	-4.3
Min	-12.4	-27.0	-7.2	-8.5	-9.3	-23.9	-5.5	-6.5
Range	3.5	3.5	2.4	2.7	0.3	0.3	1.9	2.2
SD	1.1	1.1	0.6	0.7	0.2	0.2	1.4	1.6
Mean	-11.8	-25.5	-5.2	-6.0	-10.4	-24.1	-4.7	-5.4
Max	-11.3	-25.0	-3.3	-3.9	-10.0	-23.7	-4.4	-5.1
Min	-12.6	-26.3	-6.6	-7.6	-10.7	-24.4	-4.8	-5.6
Range	1.4	1.4	3.3	3.7	0.7	0.7	0.5	0.5
SD	0.4	0.4	1.1	1.2	0.3	0.3	0.3	0.3

Table 3. Mean $\delta^{13}C$ from enamel carbonate (δ^{13}Ccarb) and diet (δ^{13}Cdiet), and $\delta^{18}O$ from enamel carbonate (δ^{18}Ocarb) and meteoric waters (δ^{18}Omw), by species on the Vasco-Cantabrian and Mediterranean areas. Max: maximum value; Min: minimum value; SD: standard deviation.

4.1 Axlor

A total of seven bovine teeth were included from levels III (n = 4), IV (n = 1), and VI (n = 2) of Axlor cave. The mean $\delta^{13}C_{carb}$ range from -8.9‰ to -9.9‰ ($\delta^{13}C_{diet}$= -23.5‰ to -24.5‰); whereas mean $\delta^{18}O_{carb}$ values are between -4.8‰ and -6.2‰ ($\delta^{18}O_{mw}$ = -5.7‰ and -7.3‰), indicating a range of variation around 1‰ and 1.4‰, respectively (Fig. 3; 4). Considering isotopic compositions by levels, mean $\delta^{13}C_{carb}$ decreases from level III to level IV, whereas mean $\delta^{18}O_{carb}$ remains stable through the sequence (Table 2; Appendix B). A range between 0.3‰ and 0.5‰ is observed in $\delta^{13}C_{carb}$ variation within tooth profiles. Individuals show clear $\delta^{18}O$ sinusoidal profiles, with peaks and troughs, and intratooth ranges from 2.1‰ to 3.4‰. The $\delta^{18}O_{mw}$ after inverse modelling intratooth profiles range from -5‰ to -6.5‰ (Appendix C; D). Mean Annual Temperatures (MATs), estimated from mean $\delta^{18}O_{mw}$ values, with seasonal control, oscillated between 10.1ºC and 14ºC (MATAs = +1-8/-2.1ºC) (Table 4). From sinusoidal profiles, summer temperatures were extracted from peaks, which are estimated to extend from 15.4ºC to 23.7ºC, and winter temperatures from troughs provided values ranging from -7ºC to 10.8ºC. Mean Annual Precipitation (MAPs), extracted from $\delta^{13}C_{carb}$, extend

https://doi.org/10.5194/bg-2023-128
Preprint. Discussion started: 9 August 2023
© Author(s) 2023. CC BY 4.0 License.

between 204mm and 326mm (MAPAs = -721/-843mm). Based on these estimations, a non-clear climatic trend is observed through these levels.

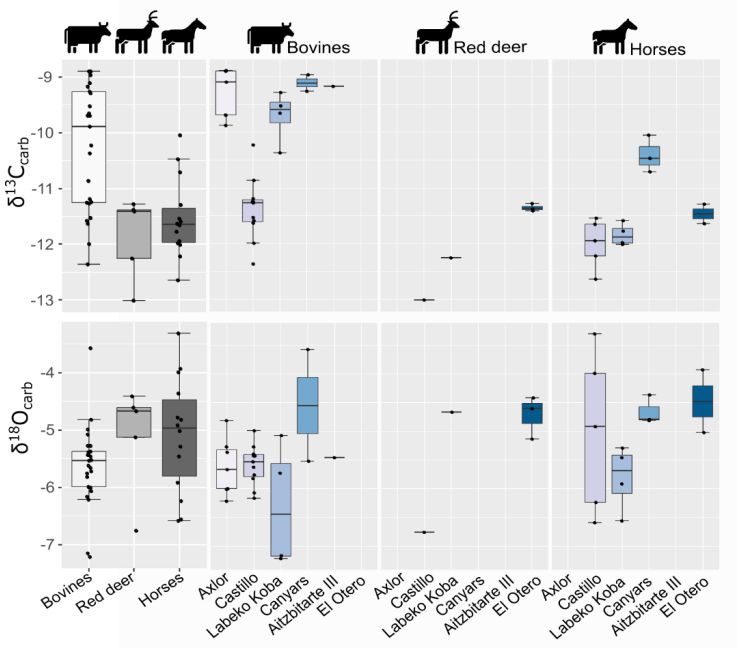

Figure 3. Distribution of mean carbon ($\delta^{13}C_{carb}$) and oxygen ($\delta^{18}O_{carb}$) isotopic values from enamel carbonate for species and archaeological site.

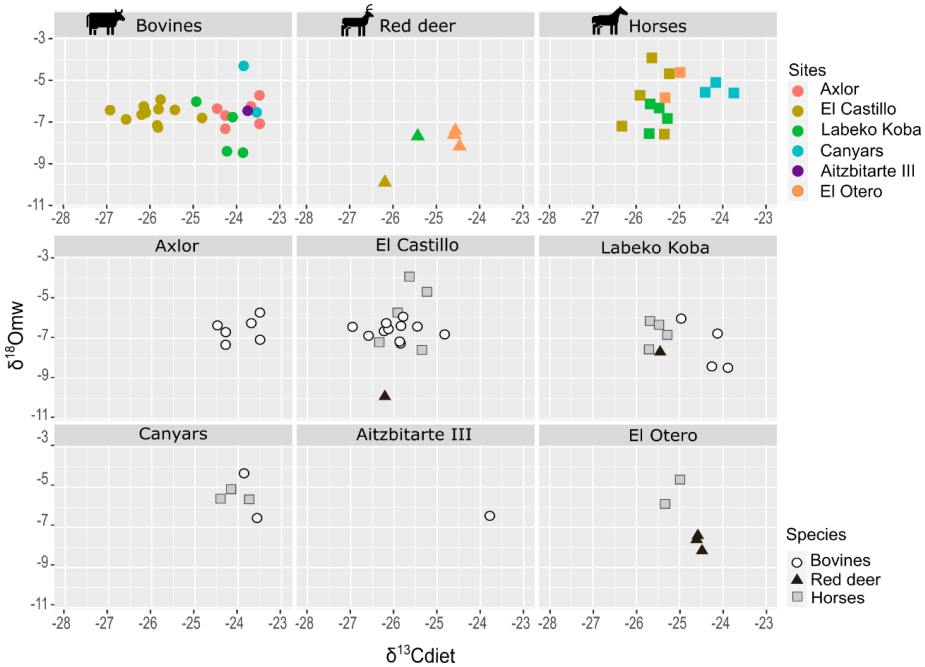

Figure 4. Biplot crossing $\delta^{13}C$ from diet and $\delta^{18}O$ from meteoric waters by species and sites.

https://doi.org/10.5194/bg-2023-128
Preprint. Discussion started: 9 August 2023
© Author(s) 2023. CC BY 4.0 License.

4.3 Labeko Koba

This work includes teeth of bovines (n = 4), horses (n = 4), and red deer (n = 1) from levels related to Châtelperronian (IXb), ProtoAurignacian (VII), and Aurignacian (VI, V, and IV). Significant differentiation in mean $\delta^{13}C_{carb}$ between bovines and horses is observed, with higher values between -9.3‰ and -10.4‰ in bovines ($\delta^{13}C_{diet}$ = -23.8‰ to -25‰) than equids, whose values extend from -11.6‰ to -12‰ ($\delta^{13}C_{diet}$ = -25.2‰ to -25.8‰) (Fig. 3;). These horses' values are within the ranges observed from this species in the region. Red deer have similar $\delta^{13}C_{carb}$ values to those of horses ($\delta^{13}C_{carb}$ = -12.3‰; $\delta^{13}C_{diet}$ = -25.5‰). Mean $\delta^{18}O_{carb}$ values are similar between species from -4.7‰ to -7.2‰ ($\delta^{18}O_{mw}$ = -6.1‰ to -8.5‰). However, bovines have a very high variation within mean $\delta^{18}O$ values (2.1‰), also reflected in the intratooth profiles. These $\delta^{18}O$ values are lower than in other Vasco-Cantabrian sites, especially for two individuals in level VII and V (Table 3). Differences in $\delta^{13}C$ values between bovines and horses result in isotopic niche differentiation between both species (Fig. 4). The red deer niche is placed within the horses' niche. The evolution of this niche over time cannot be evaluated by levels due to the limited sample. Considering the isotopic compositions by levels (Fig. 5), both bovines and horses experienced a slight increase in mean $\delta^{13}C$ from levels IXinf to IV, that is, from Châtelperronian to Aurignacian. Mean $\delta^{18}O$ values of bovines decrease from VII to V, whereas in the case of horses increase from XIinf to VI to then decrease from VI to IV.

Variability of $\delta^{13}C_{carb}$ values in intratooth profiles is slightly higher (0.1-0.7‰), especially in bovines (0.3-0.9‰), with more oscillating profiles than generally flat profiles observed in horses and red deer (Appendix C; D). Intratooth profiles ranges of $\delta^{18}O_{carb}$ are also larger within bovines (2-4‰) than in horses (1-2‰). Inverse modelled individual $\delta^{18}O_{carb}$ ranges oscillated between 5-8‰ and 2-4‰, respectively. Sinusoidal curves are observed both in horses and bovines, but bovine profiles are noisier. The red deer has a large $\delta^{18}O_{carb}$ range (6.3‰) from summer peak to an incomplete winter thought. We detect an inverse relation between $\delta^{13}C$ and $\delta^{18}O$ in some points of these individual profiles. MATs oscillated between 7ºC and 13.7ºC (MATAs = -5.6/+1.1ºC), with summer temperatures from 15.3ºC to 25ºC and winter temperatures from 0ºC to 9.1ºC. MAPs extend between 248mm and 521mm, which are notable drier conditions than nowadays (MAPAs = -798/-525mm) (Table 4). Lower rainfall levels and higher seasonal amplitudes are recorded along the sequence, especially in samples from the ProtoAurignacian level VII. Relevant differences are noticed between MAPs estimated from bovines and equids, the first providing more arid conditions.

4.4 Aitzbitarte III

A single bovine individual was analysed from level V, related to Gravettian. It has a high mean $\delta^{13}C_{carb}$ (-9.2‰) considering the observed range in bovines from the Vasco-Cantabrian region, whereas the $\delta^{18}O_{carb}$ mean value (-5.5‰) is inside the common $\delta^{18}O$ variation observed (Fig. 3). The mean $\delta^{13}C_{diet}$ value of -23.8‰ is comparable with Canyars and some individuals from Axlor, but different from Labeko Koba and El Castillo individuals. The individual $\delta^{13}C$ fluctuation is small (0.3‰) (Appendix C; D). These teeth show not quite sinusoidal profile shape in $\delta^{18}O_{carb}$, with an intratooth range of around 2.2‰. Climatic information is extracted but may be considered cautiously due to the profile shape and the limited sample size. From the inverse modelled mean $\delta^{18}O_{mw}$ value (-5.4‰), we estimate a MAT of 14.5ºC (MATA = +1.1ºC) with a summer temperature of 17.5ºC and winter temperature of 2.1ºC. The MAP estimation reached 235mm (-1127mm to nowadays) (Table 4).

4.5 El Otero

Two equids and three cervids are included from level IV from El Otero, related to the Magdalenian phase. The mean $\delta^{13}C_{carb}$ values are close, between -11.3‰ and -11.4‰ for red deer ($\delta^{13}C_{diet}$ = -24.4‰ and -24.6‰) and -11.3‰ and -11.6‰ for horse ($\delta^{13}C_{diet}$ = -25‰;-25.3‰)(Fig. 3). These $\delta^{13}C$ values for both species are relatively high concerning other studied samples, especially for cervids (around +1-2‰). Both species have higher $\delta^{18}O_{carb}$ values concerning the common range of variation observed in the Vasco-

https://doi.org/10.5194/bg-2023-128
Preprint. Discussion started: 9 August 2023
© Author(s) 2023. CC BY 4.0 License.

Cantabria region, between -3.9‰ and -5‰ for horses and between -4.4‰ and -5.1‰ for red deer. When values are transformed to $\delta^{13}C_{diet}$ and $\delta^{18}O_{mw}$, equids and cervids isotopic niches are separated (Fig. 4). All individuals show low-amplitude $\delta^{13}C_{carb}$ intratooth profiles (<0.3‰), but especially equids with an intratooth variation around 0.1‰ (Appendix C; D). Equids and cervids show $\delta^{18}O_{carb}$ sinusoidal profiles, with intratooth ranges between 1.4‰ and 2.4‰. Climatic estimations are proposed only for equids, providing MATs estimations from 13.4ºC to 16.7ºC (MATAs = -0.3ºC/+3ºC) and MAP between 400mm and 456mm (MAPAs = -755/-699mm) (Table 4). A high-temperature seasonality can be seen, with summer temperatures between 19.4ºC and 22.5ºC and winter temperatures from 0.7ºC to 7.2ºC.

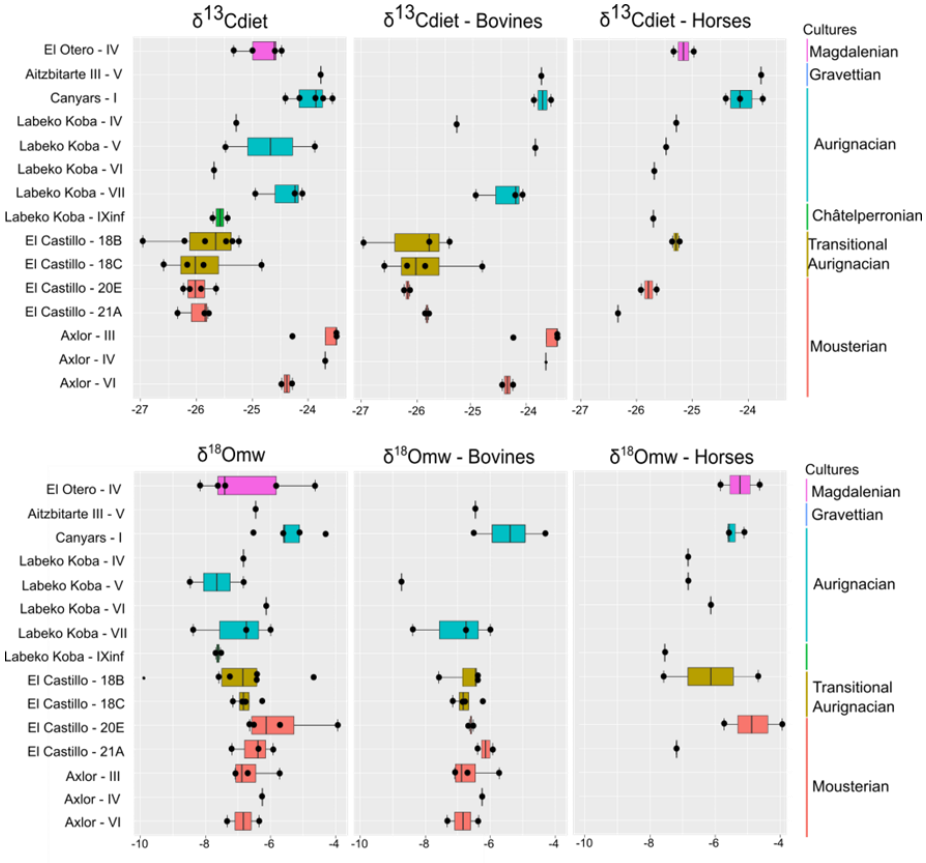

Figure 5. Evolution of $\delta^{13}C$ in diet ($\delta^{13}C_{diet}$) and $\delta^{18}O$ in meteoric waters ($\delta^{18}O_{mw}$) by archaeological levels in a diachronic order. From right to left: all species, including cervids, bovines and horses. Colors correspond to different chrono-cultures.

4.6 Canyars

From the archaeological layer I at Canyars corresponding to the Aurignacian, this work includes bovines (n = 2) and equids (n = 3) teeth. The mean $\delta^{13}C_{carb}$ values for bovines are between -9‰ to -9.3‰ ($\delta^{13}C_{diet}$ = -23.6‰ and -23.8‰), and for horses between -10‰ and -10.7‰ ($\delta^{13}C_{diet}$ = -23.7‰ and -24.4‰) (Fig.3). In this site, the $\delta^{13}C_{carb}$ values for horses are notably higher than samples in the Vasco-Cantabrian region (around +1-2‰) (Table 3). Both species have relatively high $\delta^{18}O_{carb}$ values, but they fall inside the range of variation observed in the Vasco-Cantabrian region, between -3.6‰ and -5.5‰ in bovines and between -4.4‰ and -4.8‰ in horses. Different responses are seen in mean $\delta^{18}O$ values between the two bovines,

https://doi.org/10.5194/bg-2023-128
Preprint. Discussion started: 9 August 2023
© Author(s) 2023. CC BY 4.0 License.

with one high mean value; but with close $\delta^{13}C$ mean values. Bovine and equid isotopic niches overlap (Fig. 4).

All individuals show flat $\delta^{13}C_{carb}$ intratooth profiles (<0.3‰ variation). Some individuals analysed do not show $\delta^{18}O$ sinusoidal profiles, with intratooth profiles moderately flat and ranging from 1.1‰ to 1.6‰. We detect an inverse relation between $\delta^{13}C$ and $\delta^{18}O$ in some points of bovine individual isotopic profiles. MATs oscillated between 12.5ºC and 14.8ºC (MATAs = -0.3ºC/-2.6ºC), with summer temperatures from 15.2ºC to 25.2ºC and winter temperatures from 7.3ºC to 11.4ºC (Table 4). MAPs extend between 211mm and 316mm (MAPAs = -431/-326mm). No substantial differences are noticed in the estimations based on bovines and equids because mean $\delta^{13}C$ diet values differed relatively little.

				MAT (ºC)		Summer (ºC)		Winter (ºC)		MAP (mm)	
Site	Sample	Level	Species	Estimated	Relative	Estimated	Relative	Estimated	Relative	Estimated	Relative
Axlor	AXL59	III	*Bos/Bison* sp.	10.5	-1.7	15.4	-2.6	0.9	-6.2	204	-843
Axlor	AXL60	III	*Bos/Bison* sp.	12.0	-0.2	20.4	2.5	10.8	3.7	300	-747
Axlor	AXL65	III	*Bos/Bison* sp.	10.8	-1.4	20.5	2.5	2.5	-4.6	204	-843
Axlor	AXL66	III	*Bos/Bison* sp.	14.0	1.8	20.5	2.5	1.7	-5.4	204	-843
Axlor	AXL70	IV	*Bos/Bison* sp.	12.4	0.2	19.6	1.6	-3.8	-10.9	227	-820
Axlor	AXL77	VI	*Bos/Bison* sp.	10.1	-2.1	18.2	0.2	-7.0	-14.1	300	-747
Axlor	AXL86	VI	*Bos/Bison* sp.	12.3	0.2	23.7	5.7	8.9	1.8	326	-721
El Castillo	CAS141	21A	*Bos/Bison* sp.	13.1	-0.4	22.0	3.3	4.4	-4.7	546	-486
El Castillo	CAS142	21A	*Bison priscus*	14.0	0.5	17.3	-1.3	8.9	-0.2	536	-496
El Castillo	CAS143	21A	*Equus* sp.	10.8	-2.7	20.1	1.5	5.0	-4.1	645	-387
El Castillo	CAS60	20E	*Equus* sp.					11.3	2.3	510	-522
El Castillo	CAS61	20E	*Equus* sp.	14.2	0.7	24.2	5.6	6.3	-2.8	561	-471
El Castillo	CAS139	20E	*Bos/Bison* sp.	12.5	-1.0	16.5	-2.1	7.3	-1.8	622	-410
El Castillo	CAS140	20E	*Bos/Bison* sp.	12.6	-0.9					602	-430
El Castillo	CAS135	18C	*Bos/Bison* sp.			14.8	-3.8			551	-481
El Castillo	CAS136	18C	*Bos/Bison* sp.	11.8	-1.6					699	-333
El Castillo	CAS137	18C	*Bos/Bison* sp.					5.4	-3.7	376	-656
El Castillo	CAS138	18C	*Bos/Bison* sp.	13.1	-0.4	16.1	-2.5	8.8	-0.3	612	-420
El Castillo	CAS132	18B	*Bos/Bison* sp.	11.0	-2.5	24.0	5.4	4.0	-5.1	548	-484
El Castillo	CAS133	18B	*Bos/Bison* sp.					5.2	-3.9	477	-555
El Castillo	CAS134	18B	*Bos/Bison* sp.					6.2	-2.9	784	-248
El Castillo	CAS58	18B	*Equus* sp.	9.9	-3.6	14.5	-4.1	0.1	-9.0	460	-572
El Castillo	CAS59	18B	*Equus* sp.	17.0	3.6					440	-592
Labeko Koba	LAB38	IXinf	*Equus* sp.	10.3	-2.3	15.3	-3.3	8.4	1.1	521	-526
Labeko Koba	LAB36	IV	*Equus* sp.	11.9	-0.7	16.7	-1.9	7.8	0.5	448	-599
Labeko Koba	LAB42	V	*Equus* sp.	13.1	0.5					501	-546
Labeko Koba	LAB69	V	*Bos primigenius*	7.0	-5.6	15.1	-3.5	-0.2	-7.6	248	-799
Labeko Koba	LAB20	VI	*Equus* sp.	13.7	1.1	16.2	-2.3	9.1	1.8	517	-530
Labeko Koba	LAB53	VII	*Bos primigenius*	12.5	-0.1	25.0	6.4	2.6	-4.7	278	-769
Labeko Koba	LAB55	VII	*Bos primigenius*	12.7	0.1	24.0	5.5	7.5	0.2	397	-650
Labeko Koba	LAB62	VII	*Bos/Bison* sp.	8.1	-4.5	18.3	-0.2	2.1	-5.3	295	-752
Canyars	CAN01	I	*Equus* sp.	14.3	-0.9	16.7	-5.5	11.4	2.2	232	-410
Canyars	CAN02	I	*Equus ferus*							284	-358
Canyars	CAN03	I	*Equus ferus*	14.8	-0.3	18.5	-3.7	9.5	0.3	316	-326
Canyars	CAN04	I	*Bos primigenius*			25.2	3.0			247	-395
Canyars	CAN05	I	*Bos primigenius*	12.5	-2.6	15.2	-7.0	7.3	-1.8	211	-431
Aitzbitarte III	AITI10	V	*Bos/Bison* sp.	14.5	1.1	17.5	-1.5	2.1	-6.5	235	-1127
Otero	OTE11	IV	*Equus* sp.	13.4	-0.3	19.4	0.6	0.8	-8.6	456	-699
Otero	OTE12	IV	*Equus* sp.	16.7	3.0	22.5	3.7	7.2	-2.2	400	-755

Table 4. Summary of paleoclimatic estimations, based on $\delta^{18}O$ for temperatures (Mean Annual Temperatures, MAT; summer; winter) and in $\delta^{13}C$ for precipitation (Mean Annual Precipitations, MAP). Only teeth with validated seasonal curves are included in the summer and winter temperature estimation after modelling teeth peaks and trough profiles. For some profiles with an unclear seasonal shape, MATs were deduced from the original average of teeth without a seasonal profile (values marked in red). Details on teeth selection are presented in Appendix B.

5. Discussion

5.1 Diet and ecological niches: carbon ratios

Carbon isotopic ratios are valuable indicators for discerning past animal diets based on the ecosystems where the animals most frequently foraged. Considering species trends in the studied sites, bovines have generally higher mean $\delta^{13}C$ values (from -8.9‰ to -12.4‰) than horses (from -11.3‰ to -12.6‰), whereas the red deer fall within the horses' range (from -11.3‰ to -13‰). In Canyars, in the Mediterranean area,

https://doi.org/10.5194/bg-2023-128
Preprint. Discussion started: 9 August 2023
© Author(s) 2023. CC BY 4.0 License.

bovines also show higher mean $\delta^{13}C$ values (-9‰ to -9.3‰) compared to horses (-10‰ to -10.7‰). These differentiated isotopic ranges for equids and bovines can be potentially linked to feeding behaviour, but these species are expected to present different basal $\delta^{13}C$ considering their physiology and diet. Bovines, being ruminants, have been suggested in previous studies to exhibit higher $\delta^{13}C$ values due to increased methane production (Cerling and Harris, 1999; Tejada-Lara et al., 2018). Therefore, transforming $\delta^{13}C_{carb}$ to $\delta^{13}C_{diet}$ values is crucial to mitigate the species-specific impact, particularly when comparing ruminants and non-ruminants. Bovines report $\delta^{13}C_{diet}$ values between -23.5‰ and -27.5‰ and horses between -25‰ and -26‰. These carbon compositions are typical of animals feeding on C3 plants (commonly accepted range between -34‰ and -23‰), as can be expected from high-latitude ecosystems during the Pleistocene (Cerling and Harris, 1999; Bocherens, 2003; Drucker, 2022).

Environmental factors such as light exposure, water stress, temperature fluctuations, salinity, and atmospheric CO_2 changes can influence variations in $\delta^{13}C$ values in a diet primarily based on C3 plants (Kohn, 2010; Bocherens, 2003). Typically, $\delta^{13}C_{diet}$ values below -27‰ ($\delta^{13}C_{carb}$ = -13‰) are associated with animals feeding on C3 vegetation found in closed forested environments, whereas $\delta^{13}C_{diet}$ values between -27‰ and -23‰ are linked to C3 open landscapes, which could include grasslands and steppe areas (Bocherens, 2003). The relatively high $\delta^{13}C$ observed here points to animals predominantly feeding in open environments. The canopy effect, characterised by a depletion in ^{13}C isotopes due to dense tree cover, seems unlikely among the analysed samples since none of the individuals reported $\delta^{13}C_{diet}$ below the common cut-off of -27‰ (van der Merwe, 1991; Kohn, 2010; Drucker et al., 2008). Therefore, in general terms, open mosaic landscapes, ranging from light forests to meadows and grasslands, can be inferred for northwestern Iberia. Given the generally higher $\delta^{13}C_{diet}$ values reported by bovines, it is likely that they were foraging in more open environments than horses and can be considered predominantly grazers. Particularly, bovines from El Castillo exhibit distinct feeding behavior compared to other Vasco-Cantabrian sites, as evidenced by their lower $\delta^{13}C_{diet}$ values, indicating a potential preference for browsing and feeding in closer environments, possibly in lightly forested areas. Both extinct aurochs (*Bos primigenius*) and steppe bison (*Bison priscus*) are usually classified as grass-dominant mix-feeders during the Pleistocene, although it should be noted that modern European bison (*Bison bonasus*) could include browsing in their diet (Rivals et al., 2022). For aurochs, a browse-dominated mixed feeding behaviour is also frequently described.

The $\delta^{13}C_{diet}$ range in equids indicates feeding in open environments as well, suggesting a general mix-feeding pattern for the Vasco-Cantabrian region. However, individuals from the Mediterranean area are likely grazing in more open environments, as evidenced by their notably higher $\delta^{13}C_{diet}$ values compared to the Vasco-Cantabrian region (+1-2‰). It is important to evaluate if other factors are contributing to lower $\delta^{13}C$ values in horses. In the case of equid samples from the Vasco-Cantabrian region, it should be considered that they have been pretreated with a combination of NaClO and acetic acid, which could potentially affect the isotopic values. Samples after organic removal pretreatment can potentially show either higher or lower $\delta^{13}C$ values and higher $\delta^{18}O$ values based on previous experiments (Pellegrini and Snoeck, 2016; Snoeck and Pellegrini, 2015), with $\delta^{13}C$ values generally varying below 0.3‰. Based on the observation that horses in the Vasco-Cantabrian region present lower $\delta^{13}C$ values compared to bovines but similar mean $\delta^{18}O$ value ranges, the influence of the pre-treatment on our samples is deemed to be limited. Furthermore, the high variability in $\delta^{18}O$ values at El Castillo and Labeko Koba does not correlate with a significant variation in $\delta^{13}C$ values. Based on dental wear and stable isotopes analysis, Middle and Late Pleistocene horses (*Equus ferus*) were primarily grazers, although some rare cases have been reported as mixed feeders or browsers, such as at Igue des Rameaux amont or Schöningen (Kuitems et al., 2015; Rivals et al., 2009, 2015; Uzunidis, 2020). Horse populations from northern and eastern Europe were found to be browsers or mixed feeders, while those from the Mediterranean region tend to be grazers (Rivals et al., 2022).

https://doi.org/10.5194/bg-2023-128
Preprint. Discussion started: 9 August 2023
© Author(s) 2023. CC BY 4.0 License.

Finally, the few cervids included in this study exhibit $\delta^{13}C_{diet}$ values that frequently overlap with those of horses, indicating a mixed feeding behaviour that varies from more closed environments in El Castillo to more open habitats in El Otero. During the Pleistocene, the red deer (*Cervus elaphus*) exhibit a flexible, mixed-feeding behavior, consuming leaves, shrubs, forbs, grass, and sedges, similar to their present-day counterparts (Rivals et al., 2022; Merceron et al., 2021). This species inhabits diverse habitats ranging from steppes to closed temperate forests.

5.2 Seasonality, mobility and water acquisition: oxygen ratios and intratooth profiles

Average values of $\delta^{18}O$ in Vasco-Cantabrian individuals extend between -3.3‰ and -7.2‰ (Table 3). Even if no clear species patterns in $\delta^{18}O$ are observed, in general, bovines present slightly lower $\delta^{18}O$ values from -4.8‰ to -7.2‰ than other species; horses have a large variation from -3.3‰ to -6.6‰ and red deer from -4.4‰ to -6.8‰. In Canyars, both species have relatively high $\delta^{18}O$ values that fall inside the variation range observed in the Vasco-Cantabrian region, between -3.6‰ and -5.5‰ in bovines and between -4.4‰ and -4.8‰ in horses. Each species show different $\delta^{18}O$ intratooth ranges, with bovines between 1‰ and 3‰, equids mostly around 1.5%, and cervids presenting the higher ranges, from 1‰ to 6‰ (Table 3; Appendix C). After applying inverse modelling to correct the dampening effect (Passey et al., 2005), the majority of teeth increase the $\delta^{18}O$ intratooth range, between 3‰ and 8‰ for bovines and 2‰ and 7‰ for horses (Appendix D). Most bovines from Axlor and Labeko Koba and equids from El Castillo and El Otero exhibit well-defined sinusoidal profiles in their $\delta^{18}O$ intratooth individual values, indicating potential seasonal fluctuations between $\delta^{18}O$ values of environmental summer and winter meteoric waters, although not all samples follow this pattern consistently. Certain intratooth profiles, particularly those from bovines in El Castillo and Canyars, exhibit sharp profiles with narrow ranges. This phenomenon was previously reported in the region in preliminary studies conducted at the sites of El Castillo (Jones et al., 2019) and in the Magdalenian levels of El Mirón cave (Geiling, 2020).

Non-sinusoidal profiles observed in the data can be attributed to various factors, including issues related to sample techniques and preservation and the inherent variability in the original isotopic signal. Factors related to sampling and methods can be connected to 1) the sampling process (e.g. too deep or too distant sampling grooves); 2) the imprecision of the mass spectrometer measurements; 3) uncontrolled effects of samples pretreatments; 4) diagenetic alterations affecting the carbonate fraction. However, it must be noted that technical reasons, whether related to sampling or pretreatment, do not appear to impact the obtained results significantly. First, this study reproduces the same intratooth sampling methods that previously yielded reliable results in similar research (e.g., Pederzani et al., 2023, 2021a). Second, non-significant alterations in intratooth profiles of pretreated horse samples (El Castillo, Labeko Koba, Otero) are noticed in comparison to untreated bovid samples (Appendix C). Some bovid samples are equally showing these non-sinusoidal profiles. In sites where both species are analysed, no correlation is observed between $\delta^{18}O$ and $\delta^{13}C$. In tooth enamel, diagenetic alterations are generally less pronounced than bone due to its larger mineral content. However, carbonates within tooth enamel can be more susceptible to diagenesis and recrystallisation compared to the phosphate fraction, which contains a larger reservoir of oxygen and stronger oxygen bonds (Zazzo et al., 2004; Chenery et al., 2012; Bryant et al., 1996). The carbonate content in our samples, ranging from 3.9% to 8.9%, is similar to the proportion found in modern tooth enamel, suggesting no immediate indication of diagenetic alteration. Diagenesis can also be evaluated by comparing the isotopic values of the carbonate and phosphate fractions in a sample, as there is a predictable difference between them. However, phosphate fraction measurements were still unavailable in our study. Additionally, in the case of diagenetic alteration, we would expect specimens from the same archaeological levels to be affected similarly, which is not the case.

Based on these arguments, it is suggested that the non-sinusoidal $\delta^{18}O$ signal observed in some individuals is likely attributed to the preservation of the original isotopic signature from water input. Several factors can

https://doi.org/10.5194/bg-2023-128
Preprint. Discussion started: 9 August 2023
© Author(s) 2023. CC BY 4.0 License.

explain why some teeth do not reflect a clear seasonal fluctuation, which could be related to animals' mobility or the isotopic composition of the water sources. The main factors considered in our study are 1) the high mobility of the animals analysed among ecosystems with different isotopic baselines due to large migrations; 2) the inland-coastal or short altitudinal movements through the region, which lead to the acquisition of water from sources with different isotopic signal; and 3) the acquisition of water from sources with no clear seasonal signal, such as large bodies of water, rivers, groundwaters, or meltwaters. Analyses of nitrogen and sulphur stable isotopes on ungulate bone collagen from Axlor, El Castillo and Labeko Koba (Jones et al., 2019, 2018; Pederzani et al., 2023) have already revealed large variation ranges linked to the existence of several microenvironments just in a few kilometres within the Vasco-Cantabria region. Long migrations and long hunting distances cannot solely explain these diversified values. In our study, the minimal $\delta^{13}C$ intratooth variation within individuals (<1‰) indicates limited seasonal changes in their feeding behavior that influenced the carbon isotopic composition (Appendix C). Therefore, considering the Vasco-Cantabrian diverse orography with perpendicular valleys that connect the Cantabrian Cordillera with the Atlantic Ocean through rivers over short distances (30-50 km), the availability in the past of a wide range of water sources in small areas seems highly likely. Furthermore, rivers in the region frequently contain meltwater from snow during the winter-spring months, and water springs are also common.

5.3 Regional trends and ecological niches

This study provides valuable insights despite the limited sample size at each archaeological level. It establishes a baseline of isotopic values for northern Iberia, allowing for the evaluation of regional trends. In the northwest, in the Vasco-Cantabrian region, the $\delta^{13}C_{carb}$ values obtained oscillated between -8.9‰ and -13‰ and between -3.3‰ and -7.2‰ in the case of $\delta^{18}O_{carb}$ values. These values are within the range expected, considering previous regional studies in ungulates (Lécuyer et al., 2021; Pederzani et al., 2023; Jones et al., 2019; Carvalho et al., 2022). Although oxygen variability trends are less precise, the main factor distinguishing the observed changes over time is the variation of carbon isotopic composition among species and regions. The combination of mean $\delta^{13}C_{diet}$ and $\delta^{18}O_{mw}$ values (Fig. 4; 5) accentuates disparities in ecological niche overlap between horses and bovines, whereas cervids and horses frequently exhibit shared ecological niches. The dissimilarities between bovines and horses could be attributed to shifts in feeding behavior, which may be accompanied by ecological and environmental changes, either independently or in parallel.

Upon evaluating the entire dataset by sites, the consistently lower $\delta^{13}C$ values in horses compared to bovids throughout time suggest both animals inhabited open landscapes, with bovines exhibiting a grazer preference while horses show a mix-feeding diet. Only in the Middle-to-Upper Paleolithic transition 18B and 18C levels of El Castillo, an exception is observed with lower $\delta^{13}C$ values in bovines, linked to a higher browser input due to a higher habitat in closer environments, such as open forests, similar to those inhabited by the horses. This generates a niche overlapping between horses and bovines, most likely reflecting stable conditions that could support both species in similar ecosystems. Contrarily, in the Châtelperronian and early Aurignacian levels from Labeko Koba, a clear differentiation between horses and bovines is observed, mainly in $\delta^{13}C$ values, highlighting the occupation of different landscapes by both species. This niche fractionation between species could result from resource competition derived from an unstable climatic period, where species needed to specialise to adapt to the changing conditions. Notable changes are also observed in the $\delta^{18}O$ values from Labeko Koba compared to the older El Castillo and Axlor sites, with bovines exhibiting a higher fluctuation range and the lowest values in the region. These trends are consistent with values observed on bone collagen from previous studies in the studied sites. During the Middle-to-Upper Paleolithic transition in the region, by comparing horses and red deer, a decrease in mean $\delta^{13}C$ (from -20‰ to -21‰) and $\delta^{15}N$ values (from 6‰ to 2.5 ‰) was observed in contrast to stable red deer mean $\delta^{13}C$ (Fernández-García et al., 2023; Jones et al., 2018, 2019). This decrease was already interpreted as niche

https://doi.org/10.5194/bg-2023-128
Preprint. Discussion started: 9 August 2023
© Author(s) 2023. CC BY 4.0 License.

fractionation, derived from an opening landscape, that drove equids into low-quality pastures compared to cervids. Pollen evidence in the region suggests a prevalence of steppe vegetation and low tree cover for the Châtelperronian and Aurignacian (Iriarte-Chiapusso, 2000).

In the same period, at the Mediterranean site of Canyars, higher mean $\delta^{13}C_{diet}$ are observed in both species (between -23.6‰ and -24.4‰), indicating a preference for more open landscapes by bovines and equids. The indication of open areas could be linked to the arid climatic conditions associated with the Heinrich Event 4, which coincides with the formation of the archaeological level at Canyars. This predominance of open areas coincides with the presence of typical steppe herbivore species, such as *Equus hydruntinus* and *Coelodonta antiquitatis*, the microfauna and pollen taxa, and use-wear analysis on ungulate remains identified at the site (Daura et al., 2013; López-García et al., 2022; Rivals et al., 2017). Aridity is a plausible explanation for the higher niche partitioning observed in Labeko Koba and the higher $\delta^{13}C$ values found in Canyars for both species in Aurignacian levels. The $\delta^{13}C^{diet}$ results of bovines from Aitzbitarte III during the Gravettian are consistent with the trend observed in Labeko Koba, and previous studies have already suggested this time to be notably arid and cold. Finally, in the Magdalenian level of El Otero, higher $\delta^{13}C_{diet}$ values resemble those observed in Canyars. However, this time, carbon values are related to niche partitioning between horses and red deer. In contrast, higher $\delta^{18}O$ values might indicate warmer conditions but are still associated with open landscapes in the Vasco-Cantabrian area.

5.4 Late Pleistocene climatic evolution in Northern Iberia

Carbon and oxygen isotopes were used to estimate quantitative parameters related to past temperatures and precipitation. In the case of oxygen isotopic compositions, an evaluation of environmental water composition can be addressed before approaching temperature estimations. When transformed to $\delta^{18}O_{mw}$ using species-adapted correlations, the summer $\delta^{18}O_{mw}$ values obtained from the modelled teeth range from -1‰ to -4.9‰, while the winter values range from -4.2‰ to -10.6‰. These values agree with the current $\delta^{18}O_{mw}$ range of values recorded by the IAEA station (IAEA/ WMO, 2022) in Santander (from -3.5‰ in summer to -6.6‰ in winter) and in Barcelona (from -2.2‰ in summer to -6.3‰ in winter) and the OIPC (Bowen, 2022) estimations for studied locations (from -1‰ to -9‰) (Appendix B). As observed in the present, Canyars exhibit higher mean annual $\delta^{18}O_{mw}$ values of -5.5‰, which are close to the current $\delta^{18}O_{mw}$ estimated for this location (-5.4‰). This suggests that the baseline $\delta^{18}O_{mw}$ differences between Canyars and the other sites can be primarily attributed to the Mediterranean influence rather than the Atlantic, assuming equivalent air circulation patterns in the past as experienced in the present and considering IAEA stations.

Considering this work's climatic reconstruction, temperatures are generally colder and precipitation levels are notably lower than nowadays (Table 4; Appendix B). From 80,000 to 57,000 cal BP, in the Mousterian levels of the Axlor site, temperatures are generally colder than today, but there is no clear trend observed throughout the sequence, with older levels showing higher differences between summer and winter temperatures. Rainfall estimations in these levels exhibit an unusual arid pattern, possibly affected by bovines mainly feeding in open areas. Indeed, even if the species' impact has been corrected through δ13Cdiet estimation (Tejada-Lara et al., 2018), this study observed that the influence of basal feeding behavior on rainfall estimations previously advised by Lécuyer et al. (2021) should be considered. In this case, it is not possible to isolate the effect of diet from environmental interference, but previous studies have highlighted stable climatic conditions for the site (Pederzani et al., 2023).

During the Middle-to-Upper Paleolithic transition and early Aurignacian occupations, a shift in the niche configuration of species is observed, indicating climatic perturbations. There is a decreasing trend in temperatures from the Transitional Aurignacian levels in El Castillo (18C and 18B; ca. 47,000 cal BP) to the Châtelperronian (Xinf; 42,100 cal BP) and Early Aurignacian (VII-V; from 41,136 to 38,570 cal BP) levels in Labeko Koba. Lower mean annual and winter temperatures are particularly notable in El Castillo, while

https://doi.org/10.5194/bg-2023-128
Preprint. Discussion started: 9 August 2023
© Author(s) 2023. CC BY 4.0 License.

Labeko Koba exhibits high seasonal amplitude, especially in level VII. Additionally, there is a slight decrease in rainfall and increased fluctuations from the Transitional Aurignacian levels in El Castillo (18B-18C) to the Aurignacian levels in Labeko Koba (VII-V). Previous studies in the northern Iberian region underlined an environmental and ecological shift after GS13/HE5, from 48,000 to 44,000 cal BP, based on a progressive trend to colder temperatures, aridity increase, and open environmental conditions, matching with the late Neanderthal occupations, followed by a population hiatus before the arrival of Anatomically Modern Humans (Vidal-Cordasco et al., 2022; Fernández-García et al., 2023). This episode coincides with the region's maximum extension of the glaciers and a significant decrease in plant biomass and herbivore abundance (Jiménez-Sánchez et al., 2013; Ruiz-Fernández et al., 2022). Moreover, previous isotopic analyses in the region pointed to some ecological alterations considering perturbations observed in the $\delta^{13}C$ and $\delta^{15}N$ of bone collagen (Jones et al., 2019, 2018).

When comparing the environmental reconstruction of the Aurignacian period in the Vasco-Cantabrian region (levels V-IV from Labeko Koba) and the Mediterranean region (Layer I from Canyars), which are synchronous to HE4 (39,000 BP), the study reveals notably lower rainfall levels for the Mediterranean, consistent with the feeding behavior described for animals mainly feeding in open areas. These drier conditions align with the unique climatic expectations for this period and support previous findings suggesting aridity and the predominance of open landscapes (Rivals et al., 2017; Daura et al., 2013). The temperature data indicates that Canyars experienced colder conditions, especially during the winter season, compared to the present. However, in comparison to Labeko Koba, Canyars experienced warmer conditions. As explained earlier, the Mediterranean basin had consistently higher temperatures, even during colder periods. In line with this, previous studies conducted at the site have also highlighted the persistence of Mediterranean open forests in the surroundings (Rivals et al., 2017; López-García et al., 2013).

Finally, the sites Aitzbitarte III (26,692 cal BP) and El Otero (19,303 cal BP) provided valuable climatic insights into the Vasco-Cantabrian region during the Upper Paleolithic, specifically during the Gravettian and Magdalenian periods, respectively. Considering previous research in the region, the climatic trend reported for the Aurignacian, characterised by colder and more arid conditions, was expected to continue or even intensify during the Gravettian period (Fernández-García et al., 2023; Garcia-Ibaibarriaga et al., 2019b; Lécuyer et al., 2021). Both sites exhibit lower precipitation levels compared to the present, indicating significant aridity, supported by the animals predominantly feeding in open landscapes. El Otero's higher mean annual temperatures recorded in the Magdalenian horses are consistent with a climatic amelioration following the Last Glacial Maximum (Jones et al., 2021).

5. Conclusions

This study provides a comprehensive analysis of the temporal evolution of the environment and climatic conditions in northern Iberia, spanning from the late Middle Paleolithic to the late Upper Paleolithic, this is from the GS21 to the GS2, ranging from 80,000 to 15,000 cal BP. In the Vasco-Cantabrian region, the results reveal a heterogeneous landscape characterised by an open mosaic, ranging from light forest to meadows and grasslands. This landscape reconstruction is primarily influenced by the feeding locations of the studied animals and, consequently, related to the ecosystems where hominins captured them. Despite shifts in niche configuration observed between equids and bovines, both species typically forage in open areas, with bovines showing a higher preference for grazing. Only in El Castillo, during the late Mousterian and the Transitional Aurignacian levels, bovines show unusually low $\delta^{13}C$ related to higher browsing and overlapping with horse isotopic niche. This might indicate a slightly closed mosaic landscape that could sustain both species. In contrast, only horses from Canyars exhibit a preference for grazing behavior.

Stable climatic conditions are described for Mousterian Axlor and El Castillo levels from 80,000 to 50,000 BP. However, some elements indicate some environmental perturbations initiated during the Transitional

https://doi.org/10.5194/bg-2023-128
Preprint. Discussion started: 9 August 2023
© Author(s) 2023. CC BY 4.0 License.

Aurignacian levels from El Castillo, around 48,000 BP and after HE5/GS13. After GS12 (44,200-43,300 BP), horses and bovines are potentially occupying different ecological niches during the Châteleperronian and early Aurignacian levels from Labeko Koba, pointing to a species' environmental specialisation, which can be a consequence of competition for food resources during an unstable ecological period. The climatic estimations indicate a temperature shift during this period, with a slight decrease in temperatures and evidence of fluctuations in rainfall from the Transitional Aurignacian levels of El Castillo to the early Aurignacian levels of Labeko Koba. Previous environmental studies on the region have underlined ecological stress and aridity increase around 48,000 cal BP, which could sustain this biological impoverishment. When comparing the environmental conditions during the Aurignacian period in the Mediterranean (Canyars) and the Vasco-Cantabrian region (Labeko Koba), the Mediterranean area had higher baseline temperatures but also experienced higher aridity. Animals continued to feed on open landscapes during the Gravettian and Magdalenian levels in the Vasco-Cantabrian region, represented by Aitzbitarte III and El Otero sites. However, there is evidence of a temperature recovery after the LGM at the El Otero site.

For the first time, a regional approach is obtained by measuring $\delta^{13}C$ and $\delta^{18}O$ in enamel carbonates from ungulates teeth for the late Middle and Upper Paleolithic in northern Iberia. Stable isotope composition of oxygen and carbon from ungulate teeth has provided valuable insights into the diet and foraging areas of bovines, equids, and cervids. These results, derived from this extensive sampling in the Vasco-Cantabrian, establish the basis of stable isotopic studies on teeth enamel, which were slightly explored in the region. Despite the uncertainties inherent in this work, derived from using the carbonate enamel fraction for paleoclimatic estimations, both $\delta^{18}O$ and $\delta^{13}C$ contributed to the regional climatic characterisation, including the estimation of temperatures and precipitations, as well as the seasonality range between summer and winter. The potential influence of pretreatment effects and uncontrolled diagenetic alterations on the enamel carbonate fraction has been assessed. However, further investigation using new techniques like phosphate analysis and FTIR are needed to gain more insights into sample preservation. Ongoing sulphur, hydrogen and strontium studies will provide additional information on the animal mobility patterns consumed for hominins and, therefore, landscape exploitation through this transition between late Neanderthal and early modern human groups. A more comprehensive characterisation of the baseline oxygen values in the region would also enhance the environmental interpretation of the existing data.

Appendices

Appendices A, C and D are presented after bibliography. Raw data is found in Appendix B available at https://github.com/ERC-Subsilience/Ungulate_enamel-carbonate

Code availability

R code used to perform plots and models in this manuscript can be accessed at GitHub (https://github.com/ERC-Subsilience/Ungulate_enamel-carbonate).

Data availability

The available datasets used for this article are provided in the supplementary materials (Appendix A-D).

Author contribution

A.B.M.-A. got the funding and designed the research. A.B.M.-A and M.F.-G. get the permissions for sampling in the regional museums. M.F.-G., K.B, and S.P. defined the analysis strategy. M.F.-G. analysed the data and wrote the manuscript with critical inputs from A.B.M.-A., K.B, and S.P. J.M.G., L.A., M.F.-G., and A.C. M.F.-G., L.A., J.M.G., and A.C. achieved the teeth sampling and lab sample preparation. J.D. and M.S. are

responsible for the excavations in Canyars and contribute to the discussion. All the authors revised and commented on the manuscript.

Competing interests

The contact author has declared that none of the authors has any competing interests

Acknowledgments

We acknowledge the Museo de Arqueología y Prehistoria de Cantabria (MUPAC), the Consejería de Educación, Cultura y Deporte del Gobierno de Cantabria, the Museo de Arqueología de Bizkaia (Arkeologi Museoa) and the Centro de Colecciones Patrimoniales de la Diputación Foral de Gipuzkoa (Gordailua) - Provincial Government of Guipuzkoa's Heritage Collection Centre for the access to the archaeological collections. We do appreciate the work achieved by H. Reade during the initial sampling, pretreatment and analyses of samples undertaken at the University of Cantabria and Cambridge.

Financial support

Funding for Vasco-Cantabria research was obtained from the Spanish Ministry of Science and Innovation (PID2021-125818NB-I00, HAR2017-84997-P and HAR2012-33956) and the European Research Council under the European Union's Horizon 2020 Research and Innovation Programme (grant agreement number 818299; SUBSILIENCE project). Research for Canyards was funded by the Spanish Ministry of Science and Innovation (PID2020-113960GB-100), Departament de Cultura de la Generalitat de Catalunya (CLT/2022/ARQ001SOLC/128) and AGAUR (SGR2021-00337). S.P. was supported by a German Academy of Sciences Leopoldina postdoctoral fellowship (LPDS 2021-13) during this project. M.S. benefited from financial support from a Ramon y Cajal postdoctoral grant (RYC2021-032999-I).

References

Allué, E., Martínez-Moreno, J., Roy, M., Benito-Calvo, A., and Mora, R.: Montane pine forests in NE Iberia during MIS 3 and MIS 2. A study based on new anthracological evidence from Cova Gran (Santa Linya, Iberian Pre-Pyrenees), Rev. Palaeobot. Palynol., 258, 62–72, https://doi.org/10.1016/j.revpalbo.2018.06.012, 2018.

Álvarez-Lao, D. J., Rivals, F., Sánchez-Hernández, C., Blasco, R., and Rosell, J.: Ungulates from Teixoneres Cave (Moià, Barcelona, Spain): Presence of cold-adapted elements in NE Iberia during the MIS 3, Palaeogeogr. Palaeoclimatol. Palaeoecol., 466, 287–302, https://doi.org/10.1016/j.palaeo.2016.11.040, 2017.

Balasse, M., Ambrose, S. H., Smith, A. B., and Price, T. D.: The Seasonal Mobility Model for Prehistoric Herders in the South-western Cape of South Africa Assessed by Isotopic Analysis of Sheep Tooth Enamel, J. Archaeol. Sci., 29, 917–932, https://doi.org/10.1006/jasc.2001.0787, 2002.

Bendrey, R., Vella, D., Zazzo, A., Balasse, M., and Lepetz, S.: Exponentially decreasing tooth growth rate in horse teeth: implications for isotopic analyses, Archaeometry, 57, 1104–1124, https://doi.org/10.1111/arcm.12151, 2015.

Blumenthal, S. A., Cerling, T. E., Chritz, K. L., Bromage, T. G., Kozdon, R., and Valley, J. W.: Stable isotope time-series in mammalian teeth: In situ δ18O from the innermost enamel layer, Geochim. Cosmochim. Acta, 124, 223–236, https://doi.org/10.1016/j.gca.2013.09.032, 2014.

Blumenthal, S. A., Cerling, T. E., Smiley, T. M., Badgley, C. E., and Plummer, T. W.: Isotopic records of climate seasonality in equid teeth, Geochim. Cosmochim. Acta, 260, 329–348, https://doi.org/10.1016/j.gca.2019.06.037, 2019.

Bocherens, H.: Isotopic biogeochemistry and the paleoecology of the mammoth steppe fauna, Deinsea, 91, 57–76, 2003.

Brand, W. A., Coplen, T. B., Vogl, J., Rosner, M., and Prohaska, T.: Assessment of international reference materials for isotope-ratio analysis (IUPAC Technical Report), Pure Appl. Chem., 86, 425–467, https://doi.org/10.1515/pac-2013-1023, 2014.

Britton, K., Pederzani, S., Kindler, L., Roebroeks, W., Gaudzinski-Windheuser, S., Richards, M. P., and Tütken, T.: Oxygen isotope analysis of Equus teeth evidences early Eemian and early Weichselian palaeotemperatures at the Middle Palaeolithic site of Neumark-Nord 2, Saxony-Anhalt, Germany, Quat. Sci. Rev., 226, 106029, https://doi.org/10.1016/j.quascirev.2019.106029, 2019.

Bryant, J. D., Luz, B., and Froelich, P. N.: Oxygen isotopic composition of fossil horse tooth phosphate as a record of continental paleoclimate, Palaeogeogr. Palaeoclimatol. Palaeoecol., 107, 303–316, https://doi.org/10.1016/0031-0182(94)90102-3, 1994.

Bryant, J. D., Koch, P. L., Froelich, P. N., Showers, W. J., and Genna, B. J.: Oxygen isotope partitioning between phosphate and carbonate in mammalian apatite, Geochim. Cosmochim. Acta, 60, 5145–5148, https://doi.org/10.1016/S0016-7037(96)00308-0, 1996.

Carvalho, M., Jones, E. L., Ellis, M. G., Cascalheira, J., Bicho, N., Meiggs, D., Benedetti, M., Friedl, L., and Haws, J.: Neanderthal palaeoecology in the late Middle Palaeolithic of western Iberia: a stable isotope analysis of ungulate teeth from Lapa do Picareiro (Portugal), J. Quat. Sci., 37, 300–319, https://doi.org/10.1002/jqs.3363, 2022.

https://doi.org/10.5194/bg-2023-128
Preprint. Discussion started: 9 August 2023
© Author(s) 2023. CC BY 4.0 License.

Cascalheira, J., Alcaraz-Castaño, M., Alcolea-González, J., de Andrés-Herrero, M., Arrizabalaga, A., Aura Tortosa, J. E., Garcia-Ibaibarriaga, N., and Iriarte-Chiapusso, M.-J.: Paleoenvironments and human adaptations during the Last Glacial Maximum in the Iberian Peninsula: A review, Quat. Int., 581–582, 28–51, https://doi.org/10.1016/j.quaint.2020.08.005, 2021.

Cerling, T. E. and Harris, J. M.: Carbon isotope fractionation between diet and bioapatite in ungulate mammals and implications for ecological and paleoecological studies, Oecologia, 120, 347–363, https://doi.org/10.1007/s004420050868, 1999.

Chillón, B. S., Alberdi, M. T., Leone, G., Bonadonna, F. P., Stenni, B., and Longinelli, A.: Oxygen isotopic composition of fossil equid tooth and bone phosphate: an archive of difficult interpretation, Palaeogeogr. Palaeoclimatol. Palaeoecol., 107, 317–328, https://doi.org/10.1016/0031-0182(94)90103-1, 1994.

Coplen, T. B.: Guidelines and recommended terms for expression of stable-isotope-ratio and gas-ratio measurement results, Rapid Commun. Mass Spectrom., 25, 2538–2560, https://doi.org/10.1002/rcm.5129, 2011.

Coplen, T. B., Kendall, C., and Hopple, J.: Comparison of stable isotope reference samples, Nature, 302, 236–238, https://doi.org/10.1038/302236a0, 1983.

D'Angela, D. and Longinelli, A.: Oxygen isotopes in living mammal's bone phosphate: Further results, Chem. Geol., 86, 75–82, 1990.

Dansgaard, W.: Stable isotopes in precipitation, Tellus, XVI, 436–468, 1964.

Daura, J., Sanz, M., García, N., Allué, E., Vaquero, M., Fierro, E., Carrión, J. S., López-García, J. M., Blain, H. a., Sánchez-Marco, a., Valls, C., Albert, R. M., Fornós, J. J., Julià, R., Fullola, J. M., and Zilhão, J.: Terrasses de la Riera dels Canyars (Gavà, Barcelona): The landscape of Heinrich Stadial 4 north of the "Ebro frontier" and implications for modern human dispersal into Iberia, Quat. Sci. Rev., 60, 26–48, https://doi.org/10.1016/j.quascirev.2012.10.042, 2013.

Delgado Huertas, A., Iacumin, P., Stenni, B., Sánchez Chillón, B., and Longinelli, A.: Oxygen isotope variations of phosphate in mammalian bone and tooth enamel, Geochim. Cosmochim. Acta, 59, 4299–4305, https://doi.org/10.1016/0016-7037(95)00286-9, 1995.

Drucker, D. G.: The Isotopic Ecology of the Mammoth Steppe, Annu. Rev. Earth Planet. Sci., 50, 395–418, https://doi.org/10.1146/annurev-earth-100821-081832, 2022.

Drucker, D. G., Bridault, A., Hobson, K. A., Szuma, E., and Bocherens, H.: Can carbon-13 in large herbivores reflect the canopy effect in temperate and boreal ecosystems? Evidence from modern and ancient ungulates, Palaeogeogr. Palaeoclimatol. Palaeoecol., 266, 69–82, https://doi.org/10.1016/j.palaeo.2008.03.020, 2008.

Fagoaga, A.: Aproximacion paleoclimática y paisajística durante el MIS3 a partir del estudio de los micromamíferos del yacimiento de El Salt (Alcoi, Alicante)., Universidad de Burgos, 34 pp., 2014.

Fernández-García, M., Royer, A., López-García, J. M., Bennàsar, M., Goedert, J., Fourel, F., Julien, M.-A., Bañuls-Cardona, S., Rodríguez-Hidalgo, A., Vallverdú, J., and Lécuyer, C.: Unravelling the oxygen isotope signal (δ18O) of rodent teeth from northeastern Iberia, and implications for past climate reconstructions, Quat. Sci. Rev., 218, 107–121, https://doi.org/10.1016/j.quascirev.2019.04.035, 2019.

Fernández-García, M., López-García, J. M., Royer, A., Lécuyer, C., Allué, E., Burjachs, F., Chacón, M. G., Saladié, P., Vallverdú, J., and Carbonell, E.: Combined palaeoecological methods using small-mammal assemblages to decipher environmental context of a long-term Neanderthal settlement in northeastern Iberia, Quat. Sci. Rev., 228, 106072, https://doi.org/10.1016/j.quascirev.2019.106072, 2020.

Fernández-García, M., Vidal-Cordasco, M., Jones, J. R., and Marín-Arroyo, A. B.: Reassessing palaeoenvironmental conditions during the Middle to Upper Palaeolithic transition in the Cantabrian region (Southwestern Europe), Quat. Sci. Rev., 301, 107928, https://doi.org/10.1016/j.quascirev.2022.107928, 2023.

Fick, S. E. and Hijmans, R. J.: WorldClim 2: new 1-km spatial resolution climate surfaces for global land areas, Int. J. Climatol., 37, 4302–4315, https://doi.org/10.1002/joc.5086, 2017.

Garcia-Ibaibarriaga, N., Suárez-Bilbao, A., Iriarte-Chiapusso, M. J., Arrizabalaga, A., and Murelaga, X.: Palaeoenvironmental dynamics in the Cantabrian Region during Greenland stadial 2 approached through pollen and micromammal records: State of the art, Quat. Int., 506, 14–24, https://doi.org/10.1016/j.quaint.2018.12.004, 2019a.

Garcia-Ibaibarriaga, N., Suárez-Bilbao, A., Iriarte-Chiapusso, M. J., Arrizabalaga, A., and Murelaga, X.: Palaeoenvironmental dynamics in the Cantabrian Region during Greenland stadial 2 approached through pollen and micromammal records: State of the art, Quat. Int., 506, 14–24, https://doi.org/10.1016/j.quaint.2018.12.004, 2019b.

Geiling, J. M.: Human Ecodynamics in the Late Upper Pleistocene of Northern Spain: An Archeozoological Study of Ungulate Remains from the Lower Magdalenian and other Periods in El Mirón Cave (Cantabria), Universidad de Cantabria, 734 pp., 2020.

Hoppe, K. A.: Correlation between the oxygen isotope ratio of North American bison teeth and local waters: Implication for paleoclimatic reconstructions, Earth Planet. Sci. Lett., 244, 408–417, https://doi.org/10.1016/j.epsl.2006.01.062, 2006.

Hoppe, K. A., Stover, S. M., Pascoe, J. R., and Amundson, R.: Tooth enamel biomineralisation in extant horses: implications for isotopic microsampling, Palaeogeogr. Palaeoclimatol. Palaeoecol., 206, 355–365, https://doi.org/10.1016/j.palaeo.2004.01.012, 2004.

Iacumin, P., Bocherens, H., Mariotti, A., and Longinelli, A.: Oxygen isotope analyses of co-existing carbonate and phosphate in biogenic apatite: a way to monitor diagenetic alteration of bone phosphate?, Earth Planet. Sci. Lett., 142, 1–6, https://doi.org/10.1016/0012-821X(96)00093-3, 1996.

Iriarte-Chiapusso, M. J.: El entorno vegetal del yacimiento paleolítico de Labeko Koba (Arrasate, País Vasco): análisis polínico., Labeko Koba (País Vasco). Hienas y humanos en los albores del Paleolítico Super., Munibe, 89–106, 2000.

Jiménez-Sánchez, M., Rodríguez-Rodríguez, L., García-Ruiz, J. M., Domínguez-Cuesta, M. J., Farias, P., Valero-Garcés, B., Moreno, A., Rico, M., and Valcárcel, M.: A review of glacial geomorphology and chronology in northern Spain: Timing and regional variability during the last glacial cycle, Geomorphology, 196, 50–64, https://doi.org/10.1016/j.geomorph.2012.06.009, 2013.

Jones, J. R., Richards, M. P., Straus, L. G., Reade, H., Altuna, J., Mariezkurrena, K., and Marín-Arroyo, A. B.: Changing

environments during the Middle-Upper Palaeolithic transition in the eastern Cantabrian Region (Spain): direct evidence from stable isotope studies on ungulate bones, Sci. Rep., 8, 14842, https://doi.org/10.1038/s41598-018-32493-0, 2018.

Jones, J. R., Richards, M. P., Reade, H., Bernaldo de Quirós, F., and Marín-Arroyo, A. B.: Multi-Isotope investigations of ungulate bones and teeth from El Castillo and Covalejos caves (Cantabria, Spain): Implications for paleoenvironment reconstructions across the Middle-Upper Palaeolithic transition, J. Archaeol. Sci. Reports, 23, 1029–1042, https://doi.org/10.1016/j.jasrep.2018.04.014, 2019.

Jones, J. R., Marín-Arroyo, A. B., Corchón Rodríguez, M. S., and Richards, M. P.: After the Last Glacial Maximum in the refugium of northern Iberia: Environmental shifts, demographic pressure and changing economic strategies at Las Caldas Cave (Asturias, Spain), Quat. Sci. Rev., 262, 106931, https://doi.org/10.1016/j.quascirev.2021.106931, 2021.

Kohn, M. J.: Comment: Tooth Enamel Mineralization in Ungulates: Implications for Recovering a Primary Isotopic Time-Series, by B. H. Passey and T. E. Cerling (2002), Geochim. Cosmochim. Acta, 68, 403–405, https://doi.org/10.1016/S0016-7037(03)00443-5, 2004.

Kohn, M. J.: Carbon isotope compositions of terrestrial C3 plants as indicators of (paleo)ecology and (paleo)climate, Proc. Natl. Acad. Sci., 107, 19691–19695, https://doi.org/10.1073/pnas.1004933107, 2010.

Lécuyer, C., Hillaire-Marcel, C., Burke, A., Julien, M.-A., and Hélie, J.-F.: Temperature and precipitation regime in LGM human refugia of southwestern Europe inferred from δ13C and δ18O of large mammal remains, Quat. Sci. Rev., 255, 106796, https://doi.org/10.1016/j.quascirev.2021.106796, 2021.

Leuenberger, M., Siegenthaler, U., and Langway, C.: Carbon isotope composition of atmospheric CO2 during the last ice age from an Antarctic ice core, Nature, 357, 488–490, https://doi.org/10.1038/357488a0, 1992.

López-García, J. M., Blain, H.-A., Bennàsar, M., Sanz, M., and Daura, J.: Heinrich event 4 characterised by terrestrial proxies in southwestern Europe, Clim. Past, 9, 1053–1064, https://doi.org/10.5194/cp-9-1053-2013, 2013.

López-García, J. M., Blain, H.-A., Bennàsar, M., and Fernández-García, M.: Environmental and climatic context of Neanderthal occupation in southwestern Europe during MIS3 inferred from the small-vertebrate assemblages, Quat. Int., 326–327, 319–328, https://doi.org/10.1016/j.quaint.2013.09.010, 2014.

López-García, J. M., Blain, H. A., Fagoaga, A., Bandera, C. S., Sanz, M., and Daura, J.: Environment and climate during the Neanderthal-AMH presence in the Garraf Massif mountain range (northeastern Iberia) from the late Middle Pleistocene to Late Pleistocene inferred from small-vertebrate assemblages, Quat. Sci. Rev., 288, https://doi.org/10.1016/j.quascirev.2022.107595, 2022.

Marín-Arroyo, A. B. and Sanz-Royo, A.: What Neanderthals and AMH ate: reassessment of the subsistence across the Middle–Upper Palaeolithic transition in the Vasco-Cantabrian region of SW Europe, J. Quat. Sci., 37, 320–334, https://doi.org/10.1002/jqs.3291, 2022.

Merceron, G., Berlioz, E., Vonhof, H., Green, D., Garel, M., and Tütken, T.: Tooth tales told by dental diet proxies: An alpine community of sympatric ruminants as a model to decipher the ecology of fossil fauna, Palaeogeogr. Palaeoclimatol. Palaeoecol., 562, 110077, https://doi.org/10.1016/j.palaeo.2020.110077, 2021.

van der Merwe, N. J.: Light Stable Isotopes and the Reconstruction of Prehistoric Diets, Proc. Br. Acad., 77, 247–264, 1991.

North Greenland Ice Core Project members: High-resolution record of Northern Hemisphere climate extending into the last interglacial period, Nature, 431, 147–151, https://doi.org/10.1038/nature02805, 2004.

Ochando, J., Amorós, G., Carrión, J. S., Fernández, S., Munuera, M., Camuera, J., Jiménez-Moreno, G., González-Sampériz, P., Burjachs, F., Marín-Arroyo, A. B., Roksandic, M., and Finlayson, C.: Iberian Neanderthals in forests and savannahs, J. Quat. Sci., 1–28, https://doi.org/10.1002/jqs.3339, 2021.

Passey, B. H. and Cerling, T. E.: Tooth enamel mineralisation in ungulates: implications for recovering a primary isotopic time-series, Geochim. Cosmochim. Acta, 66, 3225–3234, https://doi.org/10.1016/S0016-7037(02)00933-X, 2002.

Passey, B. H., Robinson, T. F., Ayliffe, L. K., Cerling, T. E., Sponheimer, M., Dearing, M. D., Roeder, B. L., and Ehleringer, J. R.: Carbon isotope fractionation between diet, breath CO2, and bioapatite in different mammals, J. Archaeol. Sci., 32, 1459–1470, https://doi.org/10.1016/j.jas.2005.03.015, 2005.

Pederzani, S. and Britton, K.: Oxygen isotopes in bioarchaeology: Principles and applications, challenges and opportunities, Earth-Science Rev., 188, 77–107, https://doi.org/10.1016/j.earscirev.2018.11.005, 2019.

Pederzani, S., Aldeias, V., Dibble, H. L., Goldberg, P., Hublin, J. J., Madelaine, S., McPherron, S. P., Sandgathe, D., Steele, T. E., Turq, A., and Britton, K.: Reconstructing Late Pleistocene paleoclimate at the scale of human behavior: an example from the Neandertal occupation of La Ferrassie (France), Sci. Rep., 11, 1–10, https://doi.org/10.1038/s41598-020-80777-1, 2021a.

Pederzani, S., Britton, K., Aldeias, V., Bourgon, N., Fewlass, H., Lauer, T., McPherron, S. P., Rezek, Z., Sirakov, N., Smith, G. M., Spasov, R., Tran, N. H., Tsanova, T., and Hublin, J. J.: Subarctic climate for the earliest Homo sapiens in Europe, Sci. Adv., 7, 1–11, https://doi.org/10.1126/sciadv.abi4642, 2021b.

Pederzani, S., Britton, K., Jones, J. R., Agudo Pérez, L., Geiling, J. M., and Marín-Arroyo, A. B.: Late Pleistocene Neanderthal exploitation of stable and mosaic ecosystems in northern Iberia shown by multi-isotope evidence, Quat. Res., 1–25, https://doi.org/10.1017/qua.2023.32, 2023.

Pellegrini, M. and Snoeck, C.: Comparing bioapatite carbonate pre-treatments for isotopic measurements: Part 2 — Impact on carbon and oxygen isotope compositions, Chem. Geol., 420, 88–96, https://doi.org/10.1016/j.chemgeo.2015.10.038, 2016.

Pellegrini, M., Lee-Thorp, J. A., and Donahue, R. E.: Exploring the variation of the δ18Op and δ18Oc relationship in enamel increments, Palaeogeogr. Palaeoclimatol. Palaeoecol., 310, 71–83, https://doi.org/10.1016/j.palaeo.2011.02.023, 2011.

Posth, C., Yu, H., Ghalichi, A., Rougier, H., Crevecoeur, I., Huang, Y., Ringbauer, H., Rohrlach, A. B., Nägele, K., Villalba-Mouco, V., Radzeviciute, R., Ferraz, T., Stoessel, A., Tukhbatova, R., Drucker, D. G., Lari, M., Modi, A., Vai, S., Saupe, T., Scheib, C. L., Catalano, G., Pagani, L., Talamo, S., Fewlass, H., Klaric, L., Morala, A., Rué, M., Madelaine, S., Crépin, L., Caverne, J.-B., Bocaege, E., Ricci, S., Boschin, F., Bayle, P., Maureille, B., Le Brun-Ricalens, F., Bordes, J.-G., Oxilia, G., Bortolini, E., Bignon-Lau, O., Debout, G., Orliac, M., Zazzo, A., Sparacello, V., Starnini, E., Sineo, L., van der Plicht,

https://doi.org/10.5194/bg-2023-128
Preprint. Discussion started: 9 August 2023
© Author(s) 2023. CC BY 4.0 License.

J., Pecqueur, L., Merceron, G., Garcia, G., Leuvrey, J.-M., Garcia, C. B., Gómez-Olivencia, A., Połtowicz-Bobak, M., Bobak, D., Le Luyer, M., Storm, P., Hoffmann, C., Kabaciński, J., Filimonova, T., Shnaider, S., Berezina, N., González-Rabanal, B., González Morales, M. R., Marín-Arroyo, A. B., López, B., Alonso-Llamazares, C., Ronchitelli, A., Polet, C., Jadin, I., Cauwe, N., Soler, J., Coromina, N., Rufí, I., Cottiaux, R., Clark, G., Straus, L. G., Julien, M.-A., Renhart, S., Talaa, D., Benazzi, S., Romandini, M., Amkreutz, L., Bocherens, H., Wißing, C., Villotte, S., de Pablo, J. F.-L., Gómez-Puche, M., Esquembre-Bebia, M. A., Bodu, P., Smits, L., Souffi, B., Jankauskas, R., Kozakaitė, J., Cupillard, C., Benthien, H., Wehrberger, K., Schmitz, R. W., Feine, S. C., et al.: Palaeogenomics of Upper Palaeolithic to Neolithic European hunter-gatherers, Nature, 615, 117–126, https://doi.org/10.1038/s41586-023-05726-0, 2023.

Pryor, A. J. E., Stevens, R. E., Connell, T. C. O., and Lister, J. R.: Quantification and propagation of errors when converting vertebrate biomineral oxygen isotope data to temperature for palaeoclimate reconstruction, Palaeogeogr. Palaeoclimatol. Palaeoecol., 412, 99–107, https://doi.org/10.1016/j.palaeo.2014.07.003, 2014.

Rasmussen, S. O., Bigler, M., Blockley, S. P., Blunier, T., Buchardt, S. L., Clausen, H. B., Cvijanovic, I., Dahl-Jensen, D., Johnsen, S. J., Fischer, H., Gkinis, V., Guillevic, M., Hoek, W. Z., Lowe, J. J., Pedro, J. B., Popp, T., Seierstad, I. K., Steffensen, J. P., Svensson, A. M., Vallelonga, P., Vinther, B. M., Walker, M. J. C., Wheatley, J. J., and Winstrup, M.: A stratigraphic framework for abrupt climatic changes during the Last Glacial period based on three synchronised Greenland ice-core records: Refining and extending the INTIMATE event stratigraphy, Quat. Sci. Rev., 106, 14–28, https://doi.org/10.1016/j.quascirev.2014.09.007, 2014.

Rey, K., Amiot, R., Lécuyer, C., Koufos, G. D., Martineau, F., Fourel, F., Kostopoulos, D. S., and Merceron, G.: Late Miocene climatic and environmental variations in northern Greece inferred from stable isotope compositions (δ18O, δ13C) of equid teeth apatite, Palaeogeogr. Palaeoclimatol. Palaeoecol., 388, 48–57, https://doi.org/10.1016/j.palaeo.2013.07.021, 2013.

Rivals, F., Uzunidis, A., Sanz, M., and Daura, J.: Faunal dietary response to the Heinrich Event 4 in southwestern Europe, Palaeogeogr. Palaeoclimatol. Palaeoecol., 473, 123–130, https://doi.org/10.1016/j.palaeo.2017.02.033, 2017.

Rivals, F., Bocherens, H., Camarós, E., and Rosell, J.: Diet and ecological interactions in the Middle and Late Pleistocene, in: Updating Neanderthals. Understanding Behavioural Complexity in the Late Middle Palaeolithic, 39–54, 2022.

Rozanski, K., Araguás-Araguás, L., and Gonfiantini, R.: Relation Between Long-Term Trends of Oxygen-18 Isotope Composition of Precipitation and Climate, Science (80-.).., 258, 981–985, 1992.

Rufí, I., Solés, A., Soler, J., and Soler, N.: Un diente de cría de mamut (Mammuthus primigenius Blumenbach 1799, Proboscidea) procedente del Musteriense de la Cueva de la Arbreda (Serinyà, NE de la Península Ibérica), Estud. Geológicos, 74, e079, https://doi.org/10.3989/egeol.43130.478, 2018.

Ruiz-Fernández, J., García-Hernández, C., and Gallinar Cañedo, D.: The glaciers of the Picos de Europa, in: Iberia, Land of Glaciers, Elsevier, 237–263, https://doi.org/10.1016/B978-0-12-821941-6.00012-8, 2022.

Schmitt, J., Schneider, R., Elsig, J., Leuenberger, D., Lourantou, A., Chappellaz, J., Köhler, P., Joos, F., Stocker, T. F., Leuenberger, M., and Fischer, H.: Carbon Isotope Constraints on the Deglacial CO 2 Rise from Ice Cores, Science (80-.).., 336, 711–714, https://doi.org/10.1126/science.1217161, 2012.

Skrzypek, G., Sadler, R., and Wi, A.: Reassessment of recommendations for processing mammal phosphate δ18O data for paleotemperature reconstruction, Palaeogeogr. Palaeoclimatol. Palaeoecol., 446, 162–167, https://doi.org/10.1016/j.palaeo.2016.01.032, 2016.

Snoeck, C. and Pellegrini, M.: Comparing bioapatite carbonate pre-treatments for isotopic measurements: Part 1—Impact on structure and chemical composition, Chem. Geol., 417, 394–403, https://doi.org/10.1016/j.chemgeo.2015.10.004, 2015.

Tejada-Lara, J. V., MacFadden, B. J., Bermudez, L., Rojas, G., Salas-Gismondi, R., and Flynn, J. J.: Body mass predicts isotope enrichment in herbivorous mammals, Proc. R. Soc. B Biol. Sci., 285, 20181020, https://doi.org/10.1098/rspb.2018.1020, 2018.

Trayler, R. B. and Kohn, M. J.: Tooth enamel maturation reequilibrates oxygen isotope compositions and supports simple sampling methods, Geochim. Cosmochim. Acta, 198, 32–47, https://doi.org/10.1016/j.gca.2016.10.023, 2017.

Vidal-Cordasco, M., Ocio, D., Hickler, T., and Marín-Arroyo, A. B.: Ecosystem productivity affected the spatiotemporal disappearance of Neanderthals in Iberia, Nat. Ecol. Evol., 6, 1644–1657, https://doi.org/10.1038/s41559-022-01861-5, 2022.

Zazzo, A., Bendrey, R., Vella, D., Moloney, A. P., Monahan, F. J., and Schmidt, O.: A refined sampling strategy for intra-tooth stable isotope analysis of mammalian enamel, Geochim. Cosmochim. Acta, 84, 1–13, https://doi.org/10.1016/j.gca.2012.01.012, 2012.

https://doi.org/10.5194/bg-2023-128
Preprint. Discussion started: 9 August 2023
© Author(s) 2023. CC BY 4.0 License.

Appendix A. Sites description

A1. Vasco-Cantabrian sites

Axlor (Dima, Vizcaya, País Vasco)

Axlor is a rock-shelter located in Dima (43.2706; -1.8905), with a continuous Middle Paleolithic sequence from the MIS5 to the MIS3 (DeMuro et al., 2023; Pederzani et al., 2023; Marín-Arroyo et al., 2018). It is placed on the southwestern slope of the Dima valley, with an elevation of approximately 320 m above sea level (a.s.l.), at 33 km straight from the present-day coastline, next to one of the lowest mountain passes linking the Cantabrian basins and the Alavese Plateau. The site was discovered in 1932 and initial excavations were performed by Barandiarán (1967-1974). J. M. Barandiarán undertook the excavations between 1967 and 1974, identifying eight Mousterian levels (I-VIII) (Barandiarán, 1980).

From 2000 to 2008, new excavations by González-Urquijo, Ibáñez-Estévez and Rios-Garaizar were achieved and, since 2019, these are ongoing by González-Urquijo and Lazuén. Due to the lack of chronology during Barandiarán excavations, among other aspects, work was focused on obtaining a detailed stratigraphy on the new excavation areas to correlate it with Barandiarán's levels (González-Urquijo & Ibáñez-Estévez, 2021; González Urquijo et al., 2005). The new stratigraphic sequence is roughly equivalent to the previous one, but with additional levels, not previously identified or excavated by Barandiarán. Some of these levels were deposited before Level VIII (Gómez-Olivencia et al., 2018; 2020). The Middle Paleolithic sequence extends from layers VIII to III (or from N to B-C). Levallois production is predominant in the lower levels (VI to VIII), while Quina Mousterian technocomplex does in the upper ones (from III to V) (Rios-Garaizar, 2012, 2017). New chronological data by radiocarbon and OSL methods confirm that a sequence Axlor levels VI, VIII, and VIII probably accumulated during MIS5d–a (109–82 ka), while levels D to B probably were formed during the period encompassing the start of MIS 4 (71–57 ka) through to the beginning or middle of MIS 3 (57–29 ka) (Demuro et al., 2023) and upper Level III to 46,200 ±3,000 BP, which calibrates between 45,510 cal BP and the end of the calibration curve at > 55,000 cal BP (see Pederzani et al., 2023: Fig. 1).

The archaeozoological study indicate an anthropic origin of the faunal assemblage with scarce carnivore activity documented (Altuna, 1989; Castaños, 2005; Gómez-Olivencia et al., 2018). In lower layers, the most abundant taxa are *Cervus elaphus* (VIII) and *Capra pyrenaica* (VII), while in upper layers III-V, C*ervus elaphus* is substituted by *Bos primigenious/Bison priscus* and *Equus sp*. The material included in this work comes from the faunal collection of the Barandiarán excavation currently curated at the Bizkaia Museum of Archaeology (Bilbao) where teeth were sampled and the stable isotope analyses on enamel phosphate were included in Pederzani et al. (2023).

El Castillo (Puente Viesgo, Cantabria)

El Castillo is cave located in Puente Viesgo (43.2924; -3.9656), with an elevation of approximately 195m a.s.l., at 17 km straight from the present-day coastline. The cave belongs to the karstic system that was formed in the Monte Castillo, which dominates the Pas valley. The site was discovered in 1903 by H. Alcalde del Río. H. Obermaier carried out the first excavation seasons between 1910 and 1914, when many of the archeological remains were recovered, mainly from the hall of the cave. These interventions were done under the supervision of the "Institut de Paléontologie Humaine" (IPH) and of Prince Albert I of Monaco. From 1980 to 2011; V. Cabrera and F. Bernaldo de Quirós underwent new excavations focusing on the cave entrance, on the Middle to Upper Paleolithic transitional levels, mainly 16, 18 and 20 (Cabrera-Valdes, 1984). The site has yielded an important stratigraphic sequence, composed by 26 sedimentological units

https://doi.org/10.5194/bg-2023-128
Preprint. Discussion started: 9 August 2023
© Author(s) 2023. CC BY 4.0 License.

(1-26) related to different anthropic occupational units, often separated by archeologically sterile units: Eneolithic (2), Azilian (4), Magdalenian (6 and 8), Solutrean (10), Aurignacian (12, 14, 16 and 18), Mousterian (20, 21 and 22) and Acheulean (24) (Cabrera-Valdés, 1984).

Unit 21 is mostly sterile (Cabrera Valdés, 1984; Martín-Perea et al., 2023) and it was dated by ESR yielding a mean date of 69,000 ± 9,200 years BP (Rink et al., 1997). However, Martín-Perea et al. (2023) suggested some dating uncertainty arising from the interpretation of the initial stratigraphic nomenclature. They suggest that the ESR dates provided for level 21 by Rink et al. (1997) were erroneously attributed to this unit and it might correspond to 20E indicating that below that subunit the chronology is older than 70,000 years BP (Martín-Perea et al., 2023). The Mousterian Unit 20 cave is divided into several subunits (Martín-Perea et al., 2023). In Unit 20, a cave roof collapse took place transforming the cave system into an open rock shelter. This unit contains abundant archaeological and paleontological remains. Lithic industry consistent in sidescrapers, denticulates, notches and cleavers, the majority on quartzite and presents both unifacial, bifacial discoid debitage and Levallois debitage. Unit 20E was attributed to Quina Mousterian by Sánchez-Fernández and Bernaldo De Quiros (2009) and contains a Neanderthal tooth remain (Garralda, 2005). Considering the geochronological uncertainties for dates on 20E related with Rink et al. (1997), we have decided to solely rely on ERS date of 47,000 ± 9400 BP provided by Liberda et al. (2010) for this level. Unit 20C presents clear evidence of the Mousterian lithic industry and radiocarbon dates of 48,700±3,400 uncal BP (OxA-22204) and 49,400±3,700 uncal BP (OxA-22205) (Wood et al., 2018) and mean ESR date of 42,700 ±9900 BP (Liberda et al., 2010). Level 19 is archaeologically sterile and separates Unit 20 from Unit 18 (Wood et al., 2018).

Unit 18 is divided into three parts: 18A (archaeologically sterile), 18B, and 18C. Levels 18B and 18C were classified as Transitional Aurignacian, representing a gradual transformation from the Mousterian to the Aurignacian, which is unique to El Castillo cave (Cabrera et al., 2001; Maíllo and Bernaldo de Quirós, 2010; Wood et al., 2018). The dates and the cultural attribution of these levels have been the subject of much debate (e.g. Zilhao and D'Errico, 2003; Wood et al., 2018). According to Wood et al. (2018), the last dates of these levels range between 42,000±1,500 uncal BP (OxA-22203) and 46,000±2,400 uncal BP (OxA-21973), which is much earlier than the start of the Aurignacian period in the Cantabrian region (Marín-Arroyo et al., 2018; Vidal-Cordasco et al., 2023). The lithic assemblage of Unit 18 appears to be dominated by Discoid/Levallois technology (Bernaldo de Quirós and Maíllo-Fernández, 2009) but with a high percentage of "Upper Paleolithic" pieces. Additionally, punctual bone industry, as well as pieces with incisions and engravings, were discovered in Unit 18 (Cabrera-Valdés et al., 2001). Three deciduous tooth crowns attributed to Neanderthals were found in Unit 18B (Garralda et al., 2022). Above, Unit 17 is sterile but contains scarce lithic and faunal materials, while Level 16 was attributed to the Proto-Aurignacian, with dates of 38,600±1,000 uncal BP (OxA-22200) (Wood et al., 2018).

According to Luret et al. (2020), there was a shift in hunting practices between the Late Mousterian (unit 20) and the Transitional Aurignacian (unit 18). During the Late Mousterian, hunting strategies were less specialized, and the species hunted included red deer, horses, and bovines. However, in Unit 18, a specialization in red deer hunting is observed. However, the explanation of this shift has been proposed as a response to a cultural choice or induced by climatic changes. The material included in this work comes from the faunal collection recovered during the Cabrera-Valdés and Bernaldo de Quirós excavations curated at Museo de Prehistoria y Arqueología de Cantabria (MUPAC, Santander).

Labeko Koba (Arrastre, Guipúzcoa, País Vasco)

Labeko Koba is a cave located in the Kurtzetxiki Hill (43.0619; -2.4833), at 246 m a.s.l. and 29 km straight from the present-day Atlantic coast. In 1987 and 1988, due to the construction of the Arrasate ring road, the

https://doi.org/10.5194/bg-2023-128
Preprint. Discussion started: 9 August 2023
© Author(s) 2023. CC BY 4.0 License.

site was discovered and a savage excavation was carried out (Arrizabalaga, 2000a). Unfortunately, the site was destroyed after that. The stratigraphic sequence identified nine different levels. The lower Level IX was attributed to the Châtelperronian, based on the presence of three Châtelperron points. Although there is a lack of human remains in few Cantabrian Châtelperronian sites, recent research has suggested that this techno-complex was produced by Neanderthals (Maroto et al., 2012; Rios-Garaizar et al., 2022). Level VII marks the beginning of the Aurignacian sequence, likely Proto-Aurignacian, with a lithic assemblage dominated by Dufour bladelets (Arrizabalaga, 2000a). Levels VI, V, and IV contain lithic assemblages that suggested an Early Aurignacian attribution (Arrizabalaga, 2000b; Arrizabalaga et al., 2009). This site is significant because it is one of the few sites with Châtelperronian assemblages and with both Proto-Aurignacian and Early Aurignacian separated (Arrizabalaga et al., 2009).

Initial radiocarbon dates were inconsistent with the stratigraphy of the site and much more recent than expected for the Early Upper Paleolithic (Arrizabalaga, 2000a). This incoherence was determined to be affected by taphonomic alterations (Wood et al., 2014). Later radiocarbon dates undertaken with an ultrafiltration pre-treatment provided a new regional framework for the regional Early Upper Paleolithic (Wood et al., 2014). The Châtelperronian layer is dated to 38,100±900 uncal BP (OxA-22562) and 37,400±800 uncal BP (OxA-22560). The Proto-Aurignacian levels cover a period from 36,850±800 uncal BP (OxA-21766) to 35,250±650 uncal BP (OxA-21793). The three Early Aurignacian levels are dated to 35,100±600 uncal BP (OxA-21778) for level VI, ~ 34,000 uncal BP (OxA-21767 and OxA-21779) for level V, and ~ 33,000 BP (OxA-21768 and OxA-21780) for level IV (Arrizabalaga et al., 2009).

Taphonomic studies indicate an alternation in the use of the cave between carnivores and humans, the latter ones during short occupation periods (Villaluenda et al., 2012; Ríos-Garaizar et al., 2012; Arrizabalaga et al., 2010). Labeko Koba is considered to have functioned as a natural trap where carnivores, mainly hyenas, accessed to animal carcasses. At least in the base of Labeko Koba IX, carnivore activity was higher, and they would have consumed the same prey as humans (Villaluenga et al., 2012). The presence of humans is linked to strategic use as a campsite associated with a small assemblage of lithic artifacts. The most consumed species by Châtelperronian groups were red deer, followed by the consumption of large bovids, equids, and woolly rhinoceros. During the Aurignacian period, there was some stability in human occupations, although still alternated with carnivore occupations (Arrizabalaga et al., 2010). Cold-adapted fauna such as reindeer and woolly rhinoceros were identified in association with the Châtelperronian. Reindeer were still present during the Aurignacian levels, as well as the woolly mammoth and arctic fox. The original sampling of the studied teeth by this work was performed in the San Sebastian Heritage Collection headquarters where the Guipuzcoa archaeological materials were deposited at that time.

Aitzbitarte III (Renteria, Guipúzcoa, País Vasco)

Aitzbitarte III is an archaeological site located within a karstic system comprising of nine caves in Renteria (43.270; -1.8905). The cave is situated 220 m.a.s.l. and is 10 km away from the present-day coastline. Initial archaeological interventions were carried out at the end of the 19th century by P.M. de Soraluce (Altuna, 2011). Recent excavations were initially conducted in the deep zone inside the cave between 1986 and 1993, and later focused on the cave entrance between 1994 and 2002, by J. Altuna, K. Mariezkurrena, and J. Ríos-Garaizar (Altuna et al., 2011; 2017).

While the cave's entrance area contains a sequence comprising Mousterian, Evolved Aurignacian, and Gravettian layers (Altuna et al., 2011; 2013), the stratigraphy in the inner cave presents 8 levels: level VIII (some tools with Mousterian features), VII (sterile), VIb, VIa and V (Middle Gravettian technocomplex with abundance of Noailles burins), IV-II (disturbed archaeological levels) and I (surface) (Altuna et al., 2017). Levels V have dates of 24,910 uncal BP (I-15208) and 23,230 uncal BP (Ua-2243); whereas level VI extends

https://doi.org/10.5194/bg-2023-128
Preprint. Discussion started: 9 August 2023
© Author(s) 2023. CC BY 4.0 License.

from 23,830 ± 345 uncal BP (Ua-2628) and 25,380± 430 uncal BP (Ua-2244) (Altuna, 1992; Altuna et al., 2017), with a possible outlier dated at 21,130 uncal BP (Ua-1917).

The Gravettian occupation in the inner part of the cave was originally thought to be more recent than the ones in the cave entrance. However, it was difficult to correlate the two excavation areas due to different sedimentation rates. The rich human occupations took place during a singular cold phase in the Middle Gravettian with a specialized paleoeconomy focused on the hunting of *Bos primigenius* and *Bison priscus* (85% in level VI and 68% in level V), which is unusual in the Cantabrian region mostly focused on red deer and ibex. Other ungulates present are *Cervus elaphus* and *Rupicapra rupicapra*, and to a lesser extent *Capra pyrenaica, Capreolus capreolus, Rangifer tarandus*, and *Equus ferus* (Altuna et al., 2017; Altuna & Mariezkurrena, 2020). There is a scarce representation of carnivores. The tooth studied was sampled at the Gordailua Center for Heritage Collections of the Provincial Council of Gipuzkoa.

El Otero (Secadura, Voto, Cantabria)

El Otero cave is located in Secadura (Voto) (43.3565; -3.5360), at 129 m.s.a.l and 12 km straight from the present-day coastline. Near the Matienzo valley in a coastal plain environment covered by meadows and gentle hills. The discovery was made in 1908 by Lorenzo Sierra. The site was excavated in 1963 by J. Gonzalez Echegaray and M.A. García Guinea, in two different sectors (Sala I and Sala II) with an equivalent stratigraphic sequence (González Echegaray, 1966). A total of nine levels were identified in Sala I, from level IX to level I. Levels IX and VIII were originally related to the "Aurignacian-Mousterian, based on lithics assemblages with a combination of both technocomplex features. The overlying levels VI-IV were separated by a speleothem crust (level VII) and were initially related to Aurignacian, due to the presence of end-scrappers, bone points, blades, or burins on truncation (Freeman, 1964; Rios-Garaizar, 2013). Also, perforated deer, ibex, and fox teeth were found in levels V and IV. This site lacked chronological dating methods, until a selection of material from levels VI, V and IV revealed a difference chrono-cultural attribution (Marín-Arroyo et al., 2018). Radiocarbon results yielded younger dates for such a cultural attribution and show significant stratigraphic inconsistency. Level VI gave a result of 12,415±55 (OxA-32585), two dates in Level V are 12,340±55 (OxA-32509) and 10,585±50 (OxA-32510) and a date in Level IV is 15,990±80 (OxA-32508). All these results fall into the range of the Late Upper Paleolithic (Magdalenian-Azilian initially identified in levels III-I), eliminating attribution of these levels to the Aurignacian, despite the presence of apparently characteristic artefacts.

Red deer dominate the assemblage, except for level IV where horses are more abundant. Wild boar, roe deer, and ibex are also present, but large bovids are relatively rare (González Echegaray, 1966). Level IV is the richest and most anthropogenic level, with evidence of butchering in red deer (captured in winter and early summer) and chamois (in autumn) The formation of this level involved humans and carnivores, and although certain data may suggest an anthropogenic predominance, the limited sample analyzed taphonomically and the pre-selection of preserved pieces do not allow for a definitive conclusion (Yravedra & Gómez-Castanedo, 2010). The material included in this work is curated at the Museo de Prehistoria y Arqueología de Cantabria (MUPAC, Santander).

A2. Mediterranean sites

Terrasses de la Riera dels Canyars (Gavà, Barcelona, Cataluña)

Terrasses de la Riera dels Canyars (henceforth, Canyars) is an open-air site located near Gavà (Barcelona) (41.2961;1.9797), at 28 m.s.a.l and 3 km straight from the present-day coastline. The site lies on a fluvial terrace at the confluence of Riera dels Canyars, a torrential stream between Garraf Massif, Llobregat delta

https://doi.org/10.5194/bg-2023-128
Preprint. Discussion started: 9 August 2023
© Author(s) 2023. CC BY 4.0 License.

and Riera de Can Llong (Daura et al., 2013). Archaeo-paleontological remains were discovered during quarries activities in 2005 and was complete excavated on 2007 by the *Grup de Recerca del Quaternari* (Daura and Sanz, 2006; Daura et al., 2013). This intervention determined nine lithological units. The paleontological and archaeological remains come exclusively from one unit, the middle luthitic unit (MLU), and specifically from layer I. The MLU is composed of coarse sandy clays and gravels, filling a paleochannel network named lower detrital unit (LDU) (Daura et al., 2013). Five radiocarbon dates were obtained on charcoals from layer I, which yield statistically consistent ages from 33,800 ±350 uncal BP to 34,900 ±340 uncal BP, which results in mean age of 39,600 cal BP (from 37,405 to 40,916 cal BP) (Daura et al., 2013).

The layer I of the site has yielded a rich faunal assemblage, consisting of over 5,000 remains. Among the herbivores, the most common species found are *Equus ferus*, *Bos primigenius, Equus hydruntinus*, and *Cervus elaphus* (Daura et al., 2013; Sanz-Royo et al., 2020). *Capra* sp. and *Sus scrofa are* also present, although in lower frequencies. The carnivores found at the site are also noteworthy, with *Crocuta crocuta* and *Lynx pardinus* being the most frequent. Presence of cold-adapted fauna associated to stepped environments is recorded, such as cf. *Mammuthus* sp., *Coelodonta antiquitatis*, and *Equus hydruntinus*. Small mammal analysis, pollen, and use-wear analysis have provided further evidence that a steppe-dominated landscape surrounded the Canyars site, supporting a correlation with the Heinrich Event 4, in coherence with the chronology obtained for the layer (López-García et al. 2013; 2023; Rivals et al., 2017). However, the presence of woodland is also attested by forest taxa within charcoal and pollen assemblages (Daura et al., 2013).

Taphonomic study is ongoing. But several evidences point that hyenas have played an important role in the accumulation of the faunal assemblage (Daura et al., 2013; Jimenez et al. 2019). However, sporadic human presence is documented by few human modifications found in faunal remains (cutmarks and fire alterations). Although the paucity of the lithic assemblage in the site, it shows a clear attribution to Upper Palaeolithic technocomplex, most likely the Early Aurignacian (Daura et al., 2013). Recently, it was documented a perforated bone fragment, which has been identified as a perforated board for leather production (Doyon et al., 2023). All teeth included in this work were sampled in *Laboratori de la Guixera* (Ajuntament de Casteldefels) where the material is stored.

References Appendix A

Altuna, J., Mariezkurrena, K., de la Peña, P., Rios-Garaizar, J. 2011. Ocupaciones Humanas En La Cueva de Aitzbitarte III (Renteria, País Vasco) Sector Entrada: 33.000-18.000 BP. Servicio Central de Publicaciones del Gobierno Vasco; EKOB: 11–21.

Altuna, J., Mariezkurrena, K., de la Peña, P., Rios-Garaizar, J. 2013. Los niveles gravetienses de la cueva de Aitzbitarte III (Gipuzkoa). Industrias y faunas asociadas, in: de las Heras, C., Lasheras, J.A., Arrizabalaga, Á., de la Rasilla, M. editors. Pensando El Gravetiense: Nuevos Datos Para La Región Cantábrica En Su Contexto Peninsular Y Pirenaico. Monografías Del Museo Nacional Y Centro de Investigación de Altamira, 23. Madrid: Ministerio de Educación, Cultura; pp. 184–204.

Altuna, J. & Mariezkurrena, K. 2020. Estrategias de caza en el Paleolítico superior de la Región Cantábrica. El caso de Aitzbitarte II (zona profunda de la cueva). Sagvntvm-Extra 21, Homenaje al Profesor Manuel Pérez Ripoll: 219-225.

Altuna, J., Mariezkurrena, K., Ríos Garaizar, J., & San Emeterio Gómez, A. 2017. Ocupaciones Humanas en Aitzbitarte III (País Vasco) 26.000 - 13.000 BP (zona profunda de la cueva). Servicio Central de Publicaciones del Gobierno Vasco. EKOB; 8: 348pp.

Arrizabalaga, A., 2000a. El yacimiento arqueológico de Labeko Koba (Arrasate, País Vasco). Entorno. Crónica de las investigaciones. Estratigrafía y estructuras. Cronología absoluta. In: Arrizabalaga, A., Altuna, J. (Eds.), Labeko Koba (País Vasco). Hienas y Humanos en los Albores del Paleolítico Superior, Munibe (Antropologia-Arkeologia) 52. Sociedad de Ciencias Aranzadi, San Sebastián-Donostia, pp. 15-72.

Arrizabalaga, A., 2000b. Los tecnocomplejos líticos del yacimiento arqueológico de Labeko Koba (Arrasate, País Vasco). In: Arrizabalaga, A., Altuna, J. (Eds.), Labeko Koba (País Vasco). Hienas y Humanos en los Albores del Paleolítico Superior, Munibe (Antropologia-Arkeologia) 52. Sociedad de Ciencias Aranzadi, San Sebastián-Donostia, pp. 193-343.

Arrizabalaga, A., Iriarte, E., Ríos-Garaizar, J., 2009. The Early Aurignacian in the Basque Country. Quaternary International, 207: 25–36.

https://doi.org/10.5194/bg-2023-128
Preprint. Discussion started: 9 August 2023
© Author(s) 2023. CC BY 4.0 License.

Arrizabalaga, A., Iriarte, M.J. & Villaluenga, A. 2010. Labeko Koba y Lezetxiki (País Vasco). Dos yacimientos, una problemática común. Zona Arqueológica, 13: 322-334.

Barandiarán JM. 1980. Excavaciones en Axlor. 1967- 1974. En: Barandiarán, J. M.: Obras Completas. Tomo XVII; pp. 127-384.

Bernaldo de Quirós, F., Maíllo-Fernández, J.-M. 2009. Middle to Upper Palaeolithic at Cantabrian Spain. In: Camps M, Chauhan PR (eds) A sourcebook of Palaeolithic transitions: methods, theories and interpretations. Springer, New York, pp. 341–359.

Cabrera-Valdes, V. 1984. El Yacimiento de la cueva de «El Castillo» (Puente Viesgo, Santander). Bibliotheca Praehistorica Hispana 22, C.S.I.C., 485 p.

Cabrera-Valdes, V., Maillo-Fernandez, J.M., Lloret, M., Bernaldo De Quiros, F. 2001. La transition vers le Paléolithique supérieur dans la grotte du Castillo (Cantabrie, Espagne) la couche 18. L'Anthropologie 105, pp. 505–532.

Daura, J., Sanz, M. (2006). Informe de la troballa del jaciment arqueològic "Terrasses dels Canyars" (Castelldefels-Gavà). Notificació de la descoberta i propostes d'actuació. Grup de Recerca del Quaternari, SERP, UB. Servei d'Arqueologia i Paleontologia, Departament de Cultura i Mitjans de Comunicació, Generalitat de Catalunya. Unpublished Archaeological Report.

Daura, J., Sanz, M., García, N., Allué, E., Vaquero, M., Fierro, E., Carrión, J. S., López-García, J. M., Blain, H. A., Sánchez-Marco, A., Valls, C., Albert, R. M., Fornós, J. J., Julià, R., Fullola, J. M., Zilhão, J. 2013. Terrasses de la Riera dels Canyars (Gavà, Barcelona): The landscape of Heinrich stadial 4 north of the "Ebro frontier" and implications for modern human dispersal into Iberia. Quaternary Science Reviews, 60, 26–48.

Demuro, M., Arnold, L., González-Urquijo, J., Lazuen, T., Frochoso, M. 2023. Chronological constraint of Neanderthal cultural and environmental changes in southwestern Europe: MIS 5–MIS 3 dating of the Axlor site (Biscay, Spain). Journal of Quaternary Research

Doyon, L., Faure, T., Sanz, M., Daura, J., Cassard, L., D'Errico, F., 2023. A 39,600-year-old leather punch board from Canyars, Gavà, Spain. Scientific Advances, 9. https://doi.org/10.1126/sciadv.adg0834

Freeman, L.G. 1964. Mousterian Developments in Cantabrian Spain. Ph.D. thesis. Dept. of Anthropology, University of Chicago, Chicago.

Garralda, M.D. 2005. Los Neandertales en la Península Ibérica:The Neandertals from the Iberian Peninsula. Munibe (Antropologia-Arkeologia) 57, Homenaje a Jesús Altuna. pp. 289–314.

Garralda, M.D., Madrigal, T., Zapata, J., & Rosell, J. 2022. Neanderthal deciduous tooth crowns from the Early Upper Paleolithic at El Castillo Cave (Cantabria, Spain). Archaeological and Anthropological Sciences.

Gómez-Olivencia, A., Arceredillo, D., Álvarez-Lao, D.J., Garate, D., San Pedro, Z., Castaños, P., Rios-Garaizar, J., 2014. New evidence for the presence of reindeer (Rangifer tarandus) on the Iberian Peninsula in the Pleistocene: an archaeopalaeontological and chronological reassessment. Boreas 43, 286–308.

Gómez-Olivencia, A., Sala, N., Núñez-Lahuerta, C., Sanchis, A., Arlegi, M., Rios-Garaizar, J., 2018. First data of Neandertal bird and carnivore exploitation in the Cantabrian Region (Axlor; Barandiaran excavations; Dima, Biscay, Northern Iberian Peninsula). Scienti. Rep. 8, 10551.

González Echegaray, J.G. 1966. Cueva del Otero. Excavaciones Arqueológicas en España, 53. Madrid: Ministerio de Educación Nacional Dirección General de Bellas Artes Servicio Nacional de Excavaciones.

González-Urquijo, J.E., Ibáñez-Estévez, J.J. 2001. Abrigo de Axlor (Dima). Arkeoikuska: Investigación arqueológica 2001; 2002: 90–93.

González Urquijo, J.E., Ibáñez Estévez, J.J., Rios-Garaizar, J., Bourguignon, L., Castaños Ugarte, P., Tarriño Vinagre, A. 2005. Excavaciones recientes en Axlor. Movilidad y planificación de actividades en grupos de neandertales. In: Montes Barquín R, Lasheras Corruchaga JA, editors. Actas de La Reunión Científica: Neandertales Cantábricos. Estado de La Cuestión. Monografías Del Museo Nacional Y Centro de Investigación de Altamira No 20. Madrid: Ministerio de Cultura; 2005. pp. 527–539.

Jimenez, I. J., Sanz, M., Daura, J., Gaspar, I. D., García, N. 2019. Ontogenetic dental patterns in Pleistocene hyenas (Crocuta crocuta Erxleben, 1777) and their palaeobiological implications. International Journal of Osteoarchaeology, 29, 808–821.

Liberda, J.J., Thompson, J.W., Rink, W.J., Bernaldo de Quirós, F., Jayaraman, R., Selvaretinam, K., Chancellor-Maddison, K., Volterra, V., 2010. ESR dating of tooth enamel in Mousterian layer 20, El Castillo, Spain. Geoarchaeology n/a-n/a.

López-García, J.M., Blain, H.A., Fagoaga, A., Bandera, C.S., Sanz, M., Daura, J., 2022. Environment and climate during the Neanderthal-AMH presence in the Garraf Massif mountain range (northeastern Iberia) from the late Middle Pleistocene to Late Pleistocene inferred from small-vertebrate assemblages. Quaternary Science Reviews, 288.

López-García, J. M., Blain, H.-A., Bennàsar, M., Sanz, M., Daura, J. 2013. Heinrich event 4 characterized by terrestrial proxies in southwestern Europe. Climate of the Past, 9: 1053–1064.

Luret, M., Blasco, R., Arsuaga, J.L., Baquedano, E., Pérez-González, A., Sala, N., & Aranburu, A. 2020. A multi-proxy approach to the chronology of the earliest Aurignacian at the El Castillo Cave (Spain). Journal of Archaeological Science: Reports, 33: 102339.

Maroto, J., Vaquero, M., Arrizabalaga, Á., Baena, J., Baquedano, E., Jordá, J., Julià, R., Montes, R., Van Der Plicht, J., Rasines, P., Wood, R., 2012. Current issues in late Middle Palaeolithic chronology: New assessments from Northern Iberia. Quaternary International, 247: 15–25.

https://doi.org/10.5194/bg-2023-128
Preprint. Discussion started: 9 August 2023
© Author(s) 2023. CC BY 4.0 License.

Marín-Arroyo, A.B., Rios-Garaizar, J., Straus, L.G., Jones, J.R., de la Rasilla, M., González Morales, M.R., Richards, M., Altuna, J., Mariezkurrena, K., Ocio, D., 2018. Chronological reassessment of the Middle to Upper Paleolithic transition and Early Upper Paleolithic cultures in Cantabrian Spain. PLoS One 13: 1–20.

Martín-Perea, D.M., Maíllo-Fernández, J., Marín, J., Arroyo, X., Asiaín, R., 2023. A step back to move forward: a geological re-evaluation of the El Castillo Cave Middle Palaeolithic lithostratigraphic units (Cantabria, northern Iberia). Journal of Quaternary Science, 38: 221–234.

Pederzani, S., Britton, K., Jones, J.R., Agudo Pérez, L., Geiling, J.M., Marín-Arroyo, A.B., 2023. Late Pleistocene Neanderthal exploitation of stable and mosaic ecosystems in northern Iberia shown by multi-isotope evidence. Quaternary Research: 1–25.

Rink, W.J., Schwarcz, H.P., Lee, H.K., Cabrera Valdés, V., Bernaldo de Quirós, F., Hoyos, M. 1997. ESR dating of Mousterian levels at El Castillo Cave, Cantabria, Spain. Journal of Archaeological Science, 24 (7): 593-600.

Rios-Garaizar J. 2012.Industria lítica y sociedad en la Transición del Paleolítico Medio al Superior en torno al Golfo de Bizkaia. Santander: PUbliCan - Ediciones de la Universidad de Cantabria.

Rios-Garaizar, J. 2017. A new chronological and technological synthesis for Late Middle Paleolithic of the Eastern Cantabrian Region. Quaternary International, 433: 50-63.

Rios-Garaizar, J., Arrizabalaga, A. & Villaluenga, A. 2012. Haltes de chasse du Châtelperronien de la Péninsule Ibérique: Labeko Koba et Ekain (Pays Basque Péninsulaire). L'Anthropologie, 116: 532–549.

Rios-Garaizar, J., de la Peña, P., Maillo-Fernández, J.M. 2013. El final del Auriñaciense y el comienzo del Gravetiense en la región cantábrica: una visión tecno-tipológica. In: de las Heras C., Lasheras J.A., Arrizabalaga Á., de la Rasilla M. (Eds.), Pensando El Gravetiense: Nuevos Datos Para La Región Cantábrica En Su Contexto Peninsular Y Pirenaico. Monografías Del Museo Nacional Y Centro de Investigación de Altamira, 23. Madrid: Ministerio de Educación, Cultura; pp. 369–382.

Rios-Garaizar, J., Iriarte, E., Arnold, L.J., Sánchez-Romero, L., Marín-Arroyo, A.B., San Emeterio, A., Gómez-Olivencia, A., Pérez-Garrido, C., Demuro, M., Campaña, I., Bourguignon, L., Benito-Calvo, A., Iriarte, M.J., Aranburu, A., Arranz-Otaegi, A., Garate, D., Silva-Gago, M., Lahaye, C., Ortega, I. 2022. The intrusive nature of the Châtelperronian in the Iberian Peninsula. PLoS One 17, e0265219.

Rivals, F., Uzunidis, A., Sanz, M., Daura, J., 2017. Faunal dietary response to the Heinrich Event 4 in southwestern Europe. Palaeogeogr. Palaeoclimatol. Palaeoecol. 473, 123–130.

Sanz-Royo, A., Sanz, M., Daura, J. (2020). Upper Pleistocene equids from Terrasses de la Riera dels Canyars (NE Iberian Peninsula): The presence of Equus ferus and Equus hydruntinus based on dental criteria and their implications for palaeontological identification and palaeoenvironmental reconstruction. Quaternary International, 566–567, 78–90.

Vidal-Cordasco, M., Ocio, D., Hickler, T., Marín-Arroyo, A.B., 2022. Ecosystem productivity affected the spatiotemporal disappearance of Neanderthals in Iberia. Nat. Ecol. Evol. 6, 1644–1657.

Villaluenga, A., Arrizabalaga, A. & Rios-Garaizar, J. 2012. Multidisciplinary approach to two Châtelperronian series: lower IX layer of Labeko Koba and X Level of Ekain (Basque country, Spain). Journal of Taphonomy, 10: 525–548.

Wood, R.E., Arrizabalaga, A., Camps, M., Fallon, S., Iriarte-Chiapusso, M.J., Jones, R., Maroto, J., De la Rasilla, M., Santamaría, D., Soler, J., Soler, N., Villaluenga, A., Higham, T.F.G. 2014. The chronology of the earliest Upper Palaeolithic in northern Iberia: New insights from L'Arbreda, Labeko Koba and La Viña. Journl of Human Evolution, 69: 91–109. https://doi.org/10.1016/j.jhevol.2013.12.017

Wood, R., Bernaldo de Quirós, F., Maillo-Fernández, J.M., Tejero, J.M., Neira, A., Higham, T. 2018. El Castillo (Cantabria, northern Iberia) and the Transitional Aurignacian: Using radiocarbon dating to assess site taphonomy. Quaternary International, 474: 56–70.

Yravedra, J., & Gómez-Castanedo, A. 2010. Estudio zooarqueológico y tafonómico del yacimiento del Otero (Secadura, Voto, Cantabria). Espacio, Tiempo y Forma. Serie I, Nueva época. Prehistoria y Arqueología, 3: 21-38

Zilhao, J., DErrico, F. 2003 The chronology of the Aurignacian and Transitional technocomplexes. Where do we stand? In Zilhão, J. et d'Errico, F. eds., The chronology of the Aurignacian and of the transitional technocomplexes Dating, stratigraphies, cultural implications Proceedings of Symposium 61 of the XIVth Congress of the UISPP, pp. 313–349.

https://doi.org/10.5194/bg-2023-128
Preprint. Discussion started: 9 August 2023
© Author(s) 2023. CC BY 4.0 License.

Appendix C. Intratooth curve plots

Original curves derived from enamel intratooth sampling on enamel carbonate. Provided by sites. In blue, oxygen stable isotope composition ($\delta^{18}O$), and, in brown, carbon stable isotope composition ($\delta^{13}C$). In the x-axis, the distance from Enamel Rooth Junction (ERJ). Notice that the y-axis can experience some variations between sites.

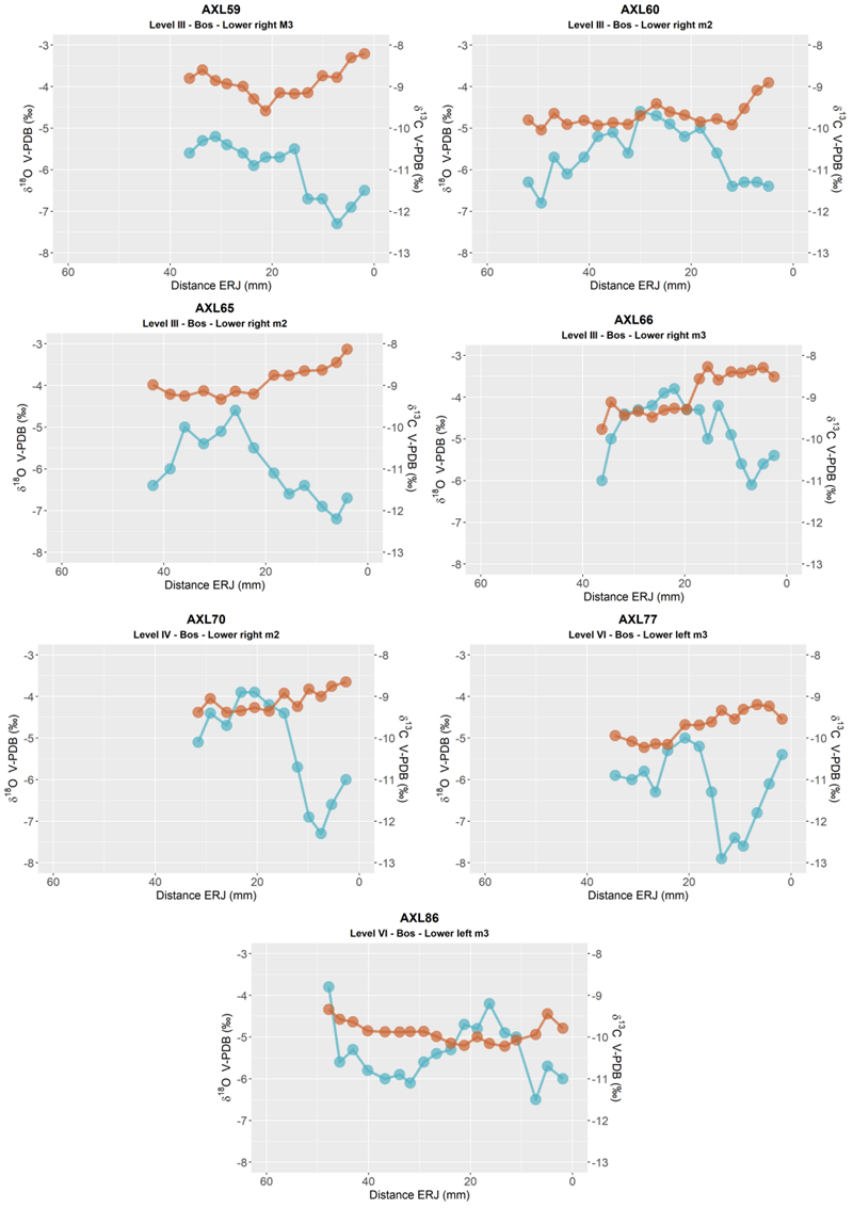

Figure C1. Intratooth plots of oxygen ($\delta^{18}O$) and carbon ($\delta^{13}C$) isotope composition from teeth from Axlor, considering distance from enamel root junction (ERC).

https://doi.org/10.5194/bg-2023-128
Preprint. Discussion started: 9 August 2023
© Author(s) 2023. CC BY 4.0 License.

Biogeosciences Discussions
Open Access
EGU

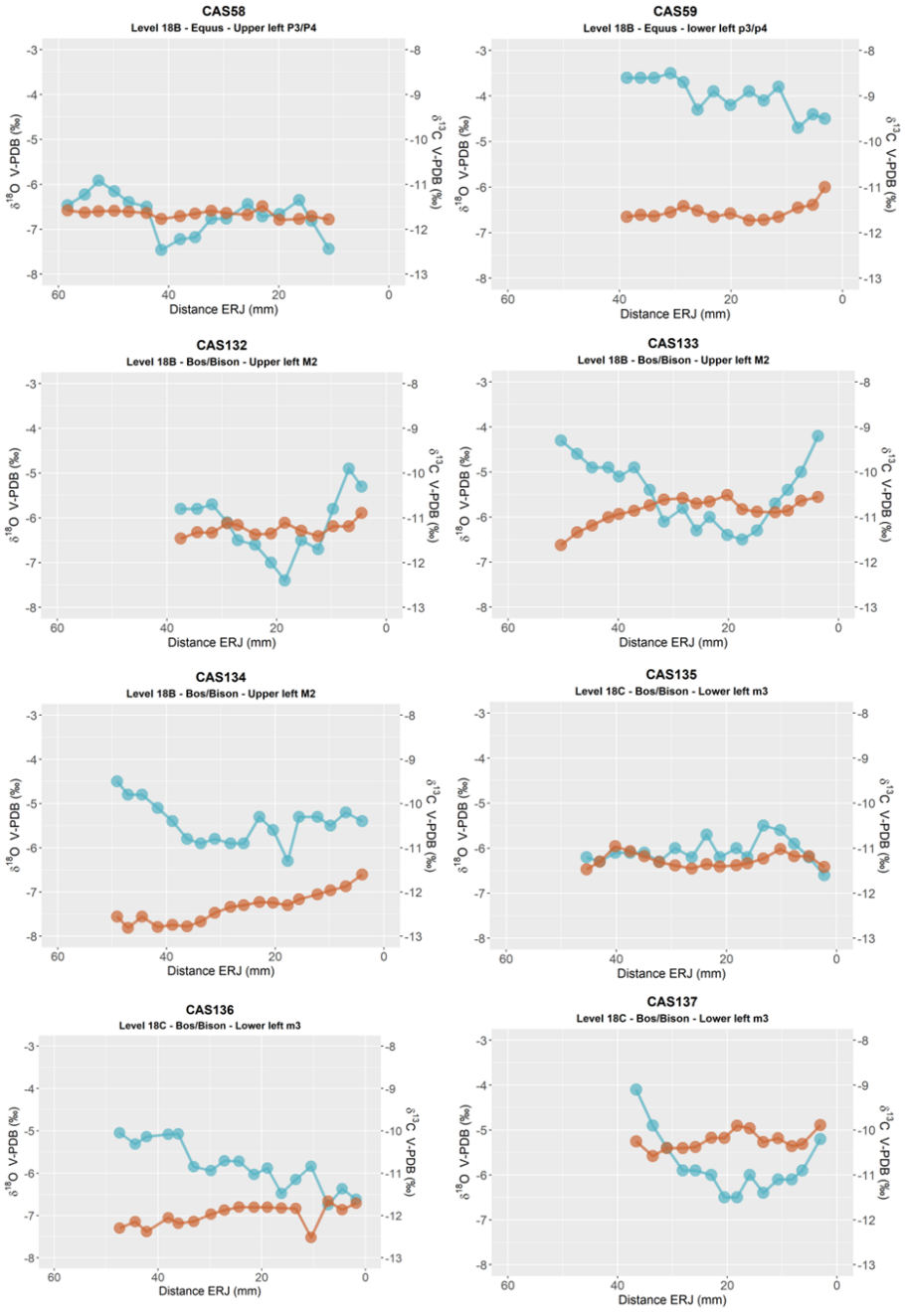

Figure C2. Intratooth plots of oxygen ($\delta^{18}O$) and carbon ($\delta^{13}C$) isotope composition from teeth from El Castillo, considering the sample's distance from the enamel root junction (ERC).

https://doi.org/10.5194/bg-2023-128
Preprint. Discussion started: 9 August 2023
© Author(s) 2023. CC BY 4.0 License.

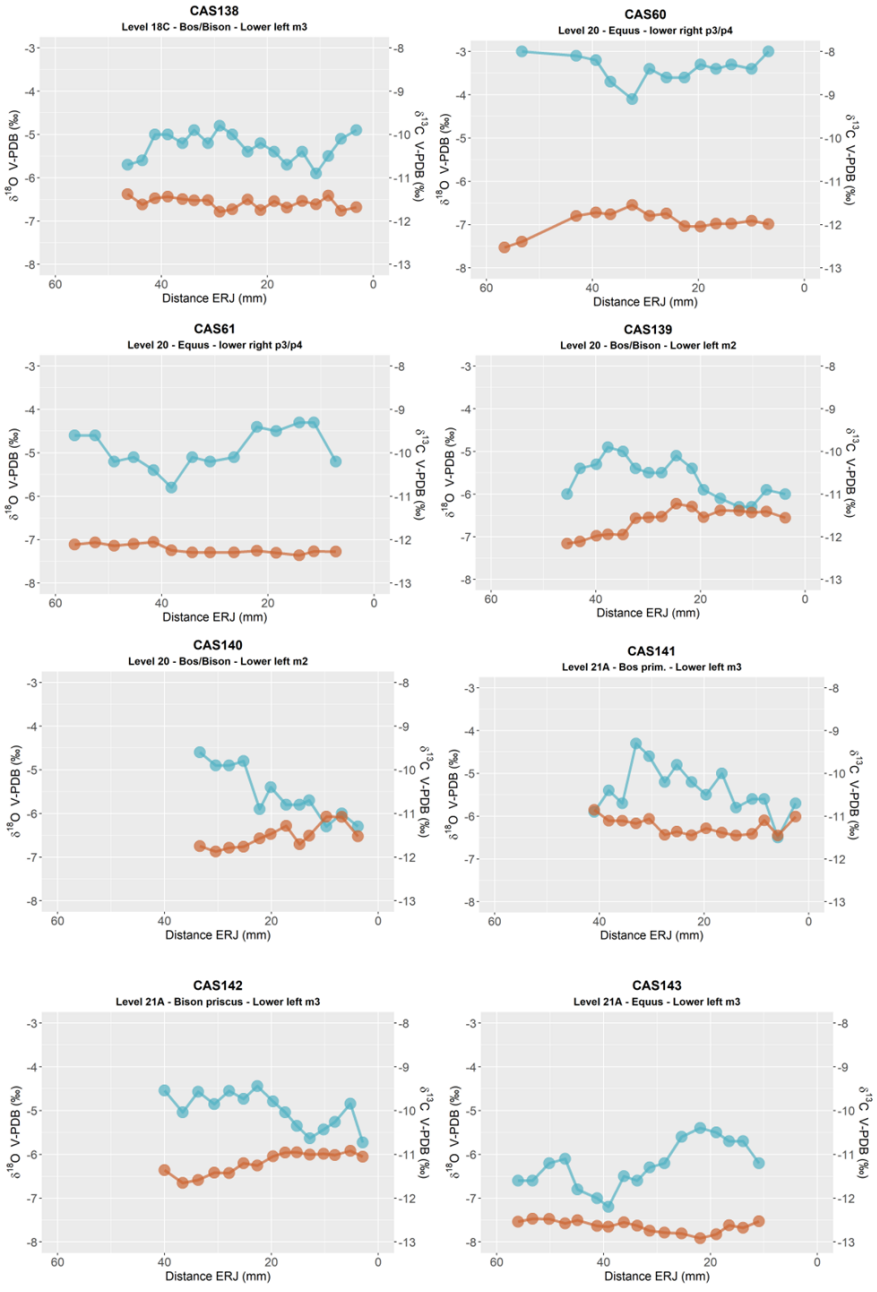

Figure C3. Intratooth plots of oxygen ($\delta^{18}O$) and carbon ($\delta^{13}C$) isotope composition from teeth from El Castillo, considering the sample's distance from the enamel root junction (ERC).

https://doi.org/10.5194/bg-2023-128
Preprint. Discussion started: 9 August 2023
© Author(s) 2023. CC BY 4.0 License.

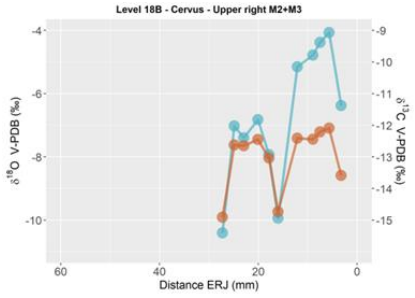

Figure C4. Intratooth plots of oxygen ($\delta^{18}O$) and carbon ($\delta^{13}C$) isotope composition from teeth from El Castillo, considering the sample's distance from the enamel root junction (ERC).

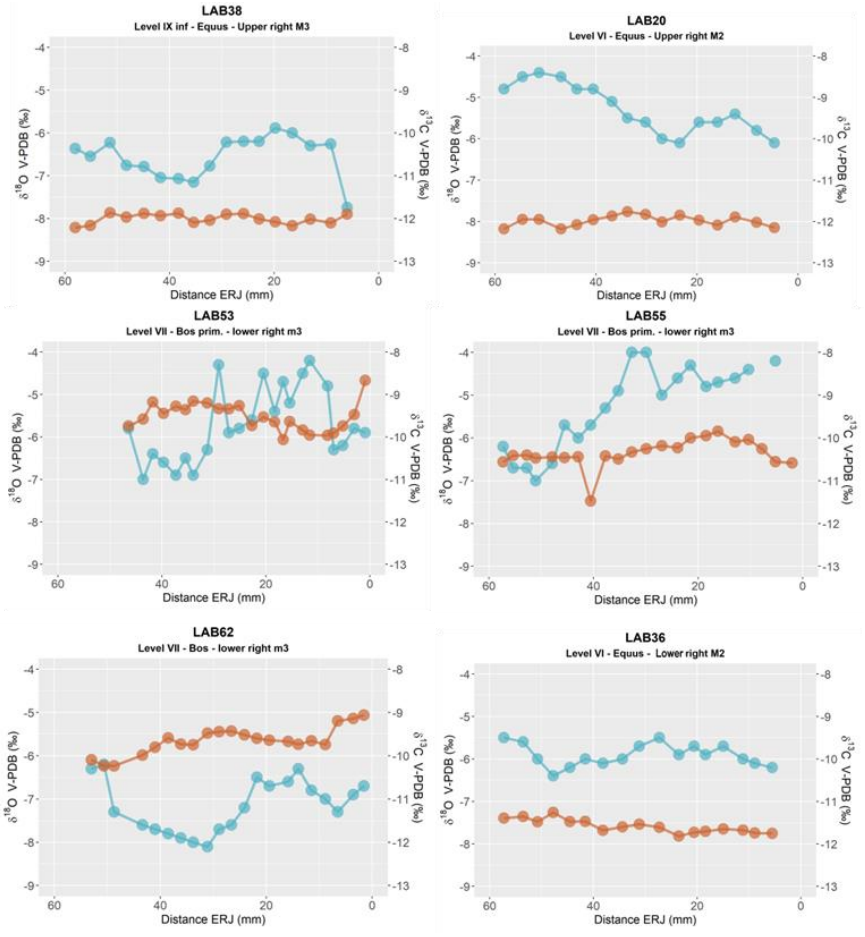

Figure C5. Intratooth plots of oxygen ($\delta^{18}O$) and carbon ($\delta^{13}C$) isotope composition from teeth from Labeko Koba, considering the sample's distance from the enamel root junction (ERC).

https://doi.org/10.5194/bg-2023-128
Preprint. Discussion started: 9 August 2023
© Author(s) 2023. CC BY 4.0 License.

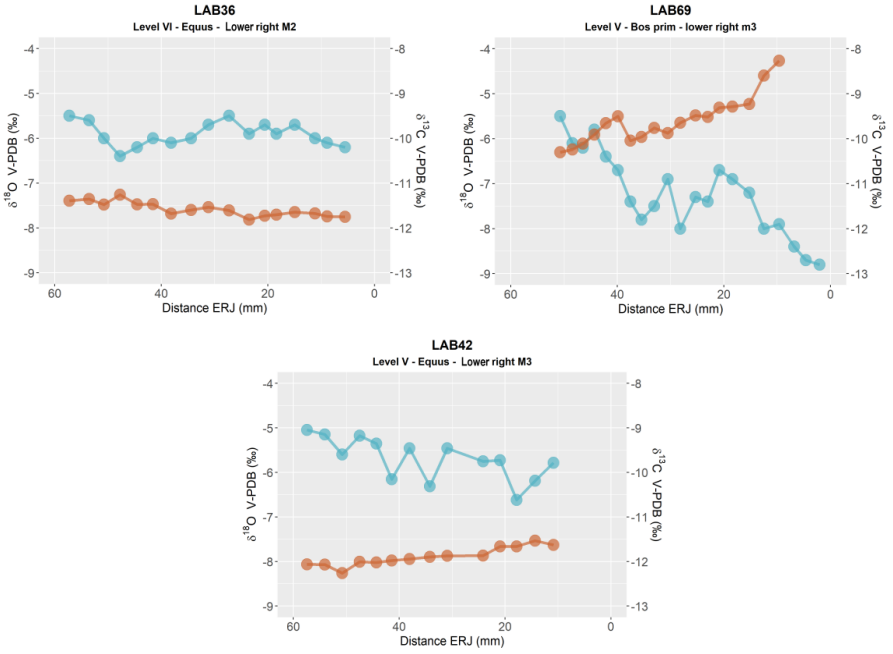

Figure C6. Intratooth plots of oxygen ($\delta^{18}O$) and carbon ($\delta^{13}C$) isotope composition from teeth from Labeko Koba, considering the sample's distance from the enamel root junction (ERC).

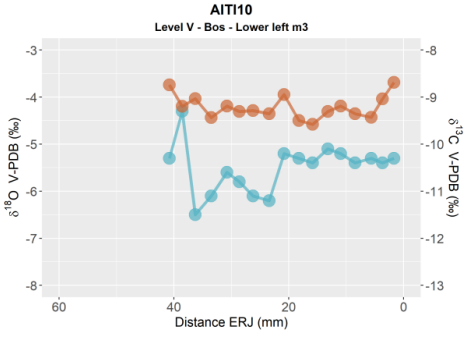

Figure C7. Intratooth plots of oxygen ($\delta^{18}O$) and carbon ($\delta^{13}C$) isotope composition from teeth from Aitzbitarte III, considering the sample's distance from the enamel root junction (ERC).

https://doi.org/10.5194/bg-2023-128
Preprint. Discussion started: 9 August 2023
© Author(s) 2023. CC BY 4.0 License.

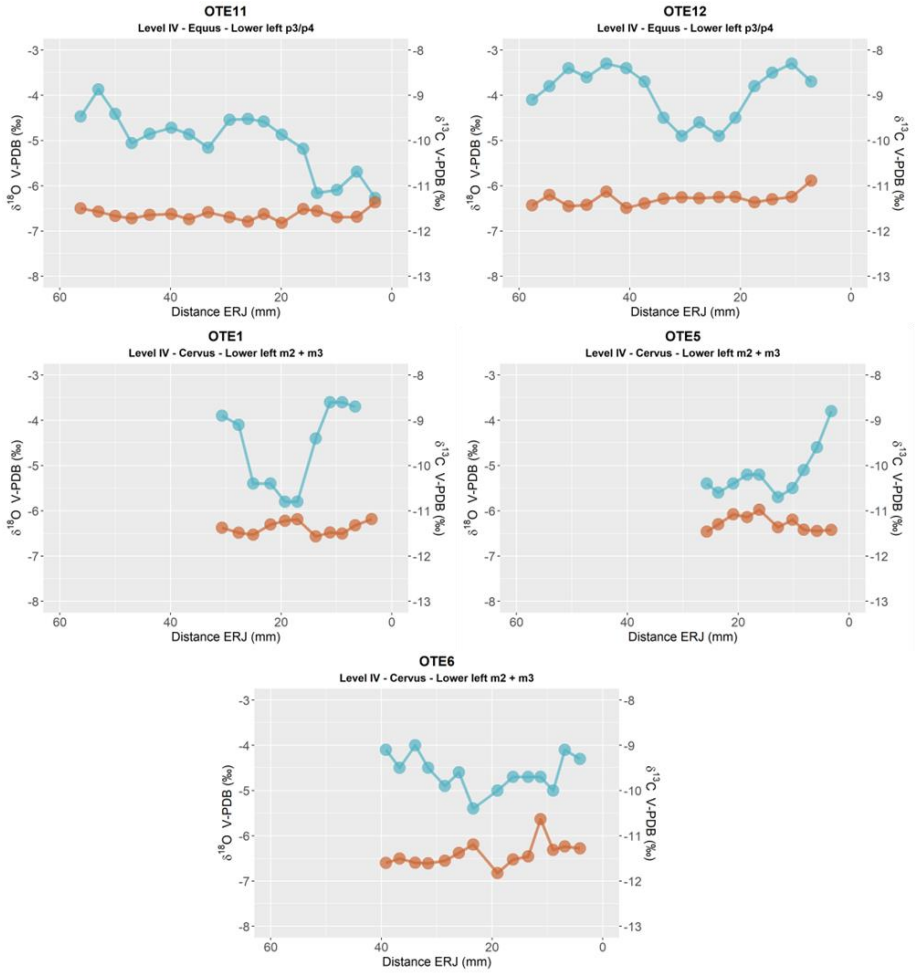

Figure C8. Intratooth plots of oxygen ($\delta^{18}O$) and carbon ($\delta^{13}C$) isotope composition from teeth from El Otero, considering the sample's distance from the enamel root junction (ERC).

https://doi.org/10.5194/bg-2023-128
Preprint. Discussion started: 9 August 2023
© Author(s) 2023. CC BY 4.0 License.

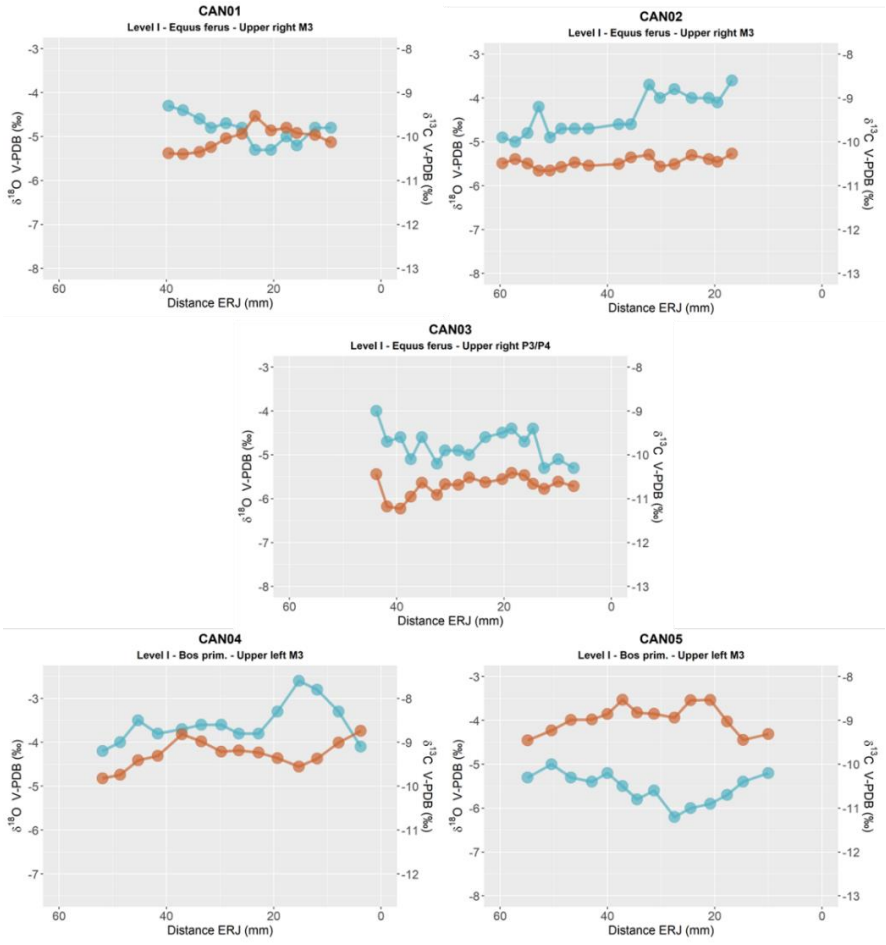

Figure C9. Intratooth plots of oxygen ($\delta^{18}O$) and carbon ($\delta^{13}C$) isotope composition from teeth from Canyars considering the sample's distance from the enamel root junction (ERC).

https://doi.org/10.5194/bg-2023-128
Preprint. Discussion started: 9 August 2023
© Author(s) 2023. CC BY 4.0 License.

Appendix D. Inverse Modelling: Methodological Details and Models

The intratooth $\delta^{18}O$ profiles presented in this study were obtained through the application of inverse modelling, using an adapted version of the code published in reference (Passey et al., 2005). This modeling approach allowed for the correction of the damping effect and the reconstruction of the original δ18O input time series. The model utilizes different species-specific parameters related to enamel formation, which vary between bovines and equids. These parameters have been established based on previous studies (Bendrey et al., 2015; Blumenthal et al., 2014; Kohn, 2004; Passey and Cerling, 2002; Zazzo et al., 2012). For Bos/Bison sp., the initial mineral content of enamel is fixed at 25%, the enamel appositional length is set at 1.5 mm, and the maturation length is 25 mm. For *Equus* sp., the initial mineral content of enamel is fixed at 22%, the enamel appositional length is set at 6 mm, and the maturation length is 28 mm.

In addition, the model requires other variables related to sampling geometry, as well as error estimates derived from mass spectrometer measurements. The distance between samples varies for each tooth, but as a general trend, the sampling depth on the tooth enamel surface in the samples of this study represents approximately 70% of the total enamel depth. The standard deviation of the measurements obtained from the mass spectrometer was typically set at 0.12%, taking into account the uncertainty associated with the standards. Finally, the models require a damping factor that determines the cumulative damping along the isotopic profile by adjusting the measured error (Emeas) to the prediction error (Epred). In the teeth analysed in this study, the damping factor ranged from 0.001 to 0.1. The most likely model solutions were selected, and summer and winter values were extracted from the $\delta^{18}O$ profiles, considering the original peaks and troughs identified in the unmodelled $\delta^{18}O$ profile. This approach was adopted to prevent the introduction of artificial peaks that the model may produce, particularly in teeth without a distinct sinusoidal shape.

https://doi.org/10.5194/bg-2023-128
Preprint. Discussion started: 9 August 2023
© Author(s) 2023. CC BY 4.0 License.

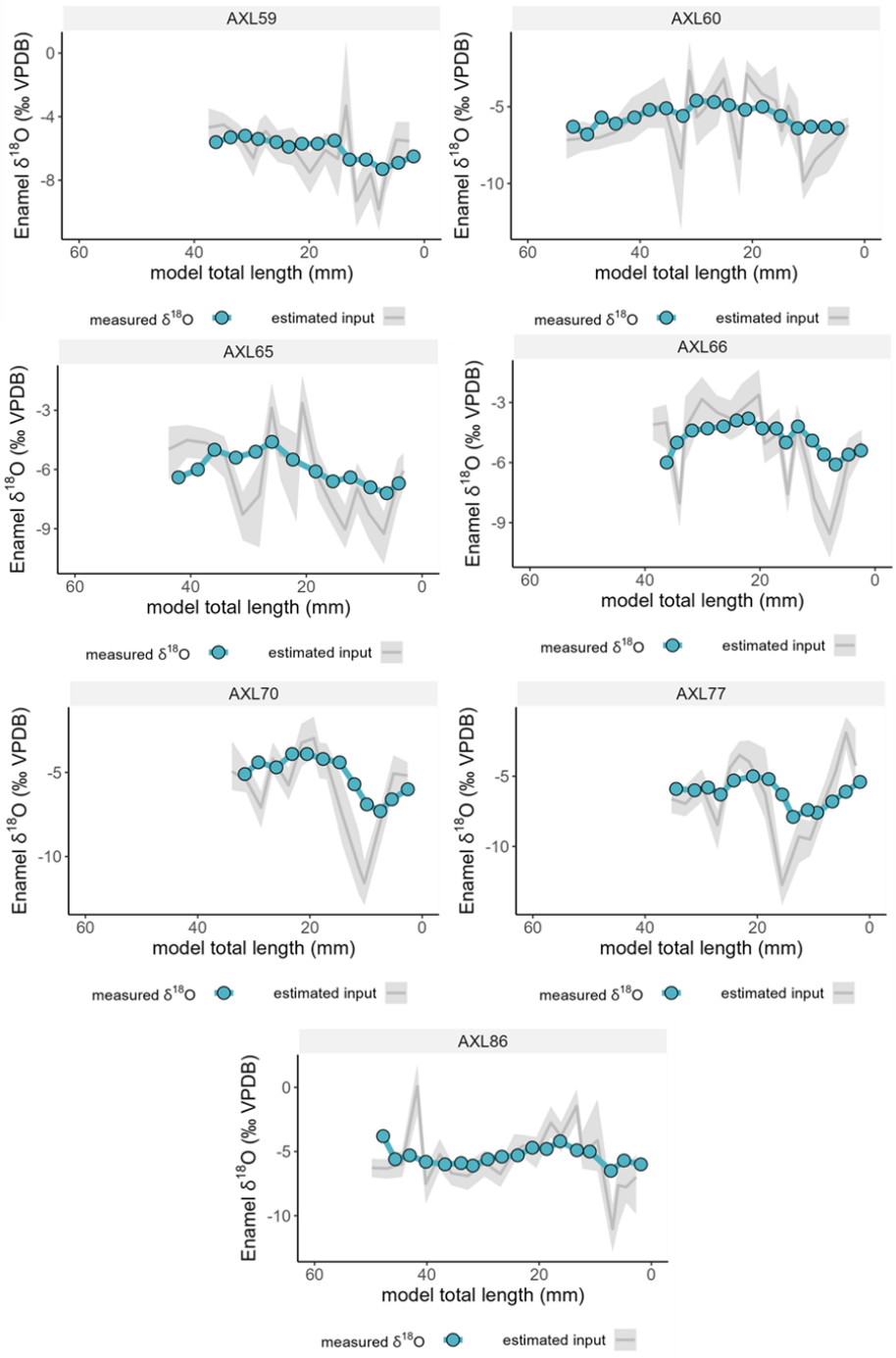

Figure D1. Inverse models for oxygen isotope composition ($\delta^{18}O$) from teeth from Axlor, considering distance from enamel root junction. The blue line and points correspond to original data and grey line the most likely model solution, with the 95% confidence interval shown in shaded areas.

https://doi.org/10.5194/bg-2023-128
Preprint. Discussion started: 9 August 2023
© Author(s) 2023. CC BY 4.0 License.

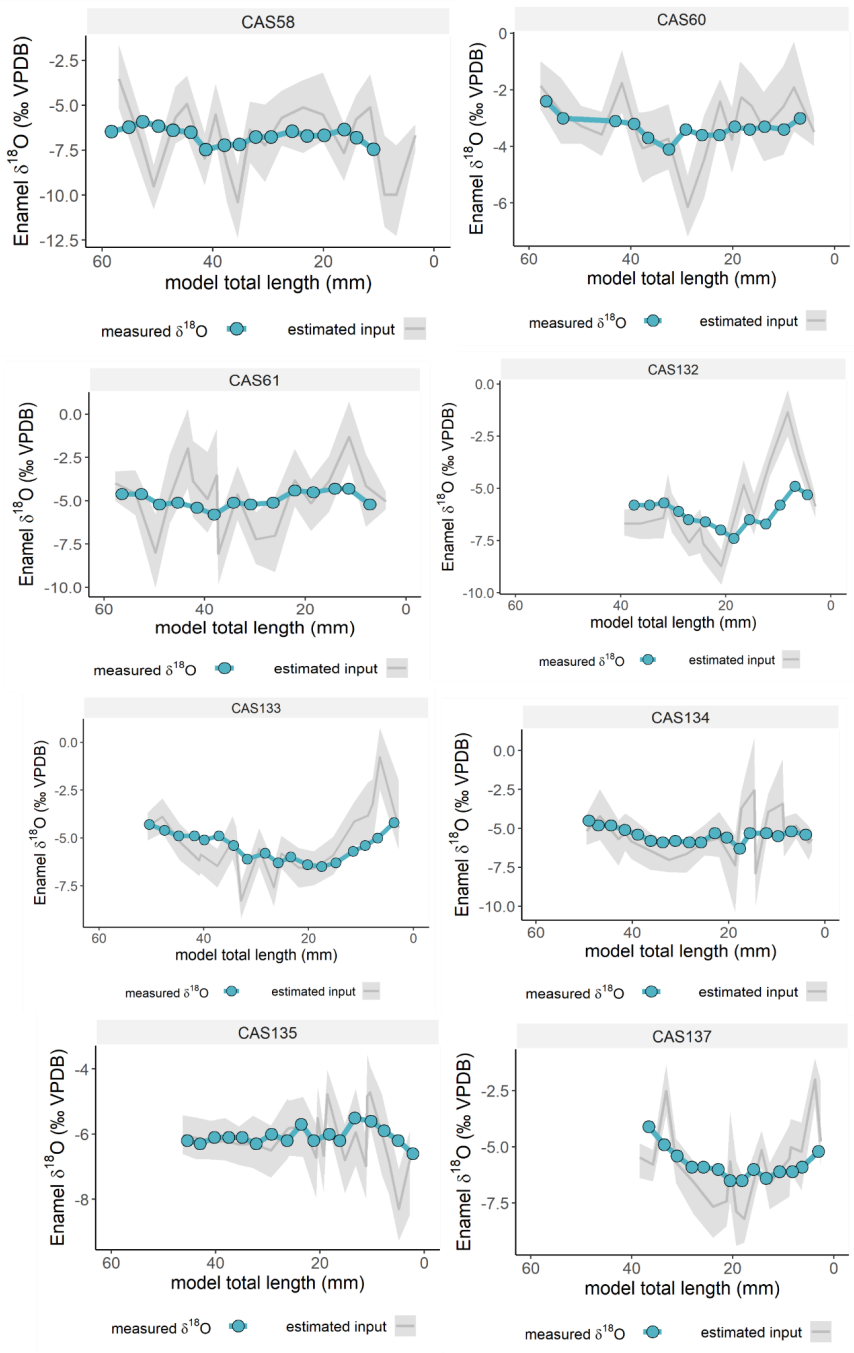

Figure D2. Inverse models for oxygen isotope composition ($\delta^{18}O$) from teeth from El Castillo, considering distance from enamel root junction. The blue line and points correspond to original data and grey line the most likely model solution, with the 95% confidence interval shown in shaded areas.

https://doi.org/10.5194/bg-2023-128
Preprint. Discussion started: 9 August 2023
© Author(s) 2023. CC BY 4.0 License.

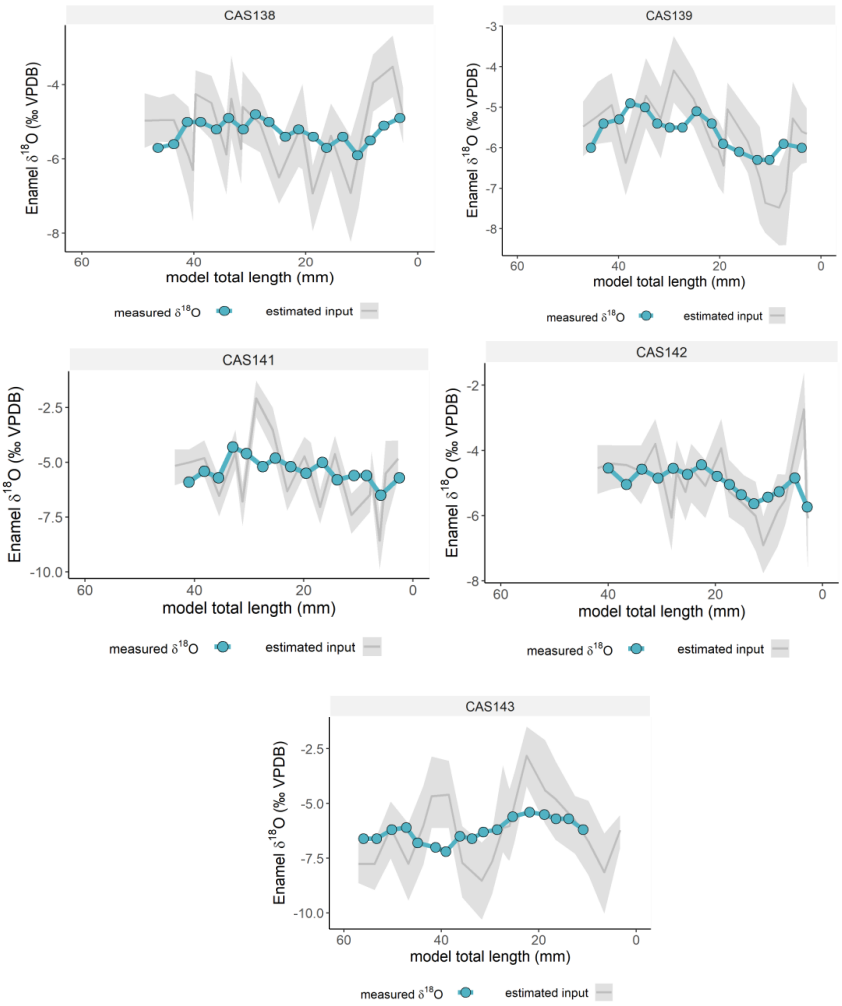

Figure D3. Inverse models for oxygen isotope composition ($\delta^{18}O$) from teeth from El Castillo, considering distance from enamel root junction. The blue line and points correspond to original data and grey line the most likely model solution, with the 95% confidence interval shown in shaded areas.

https://doi.org/10.5194/bg-2023-128
Preprint. Discussion started: 9 August 2023
© Author(s) 2023. CC BY 4.0 License.

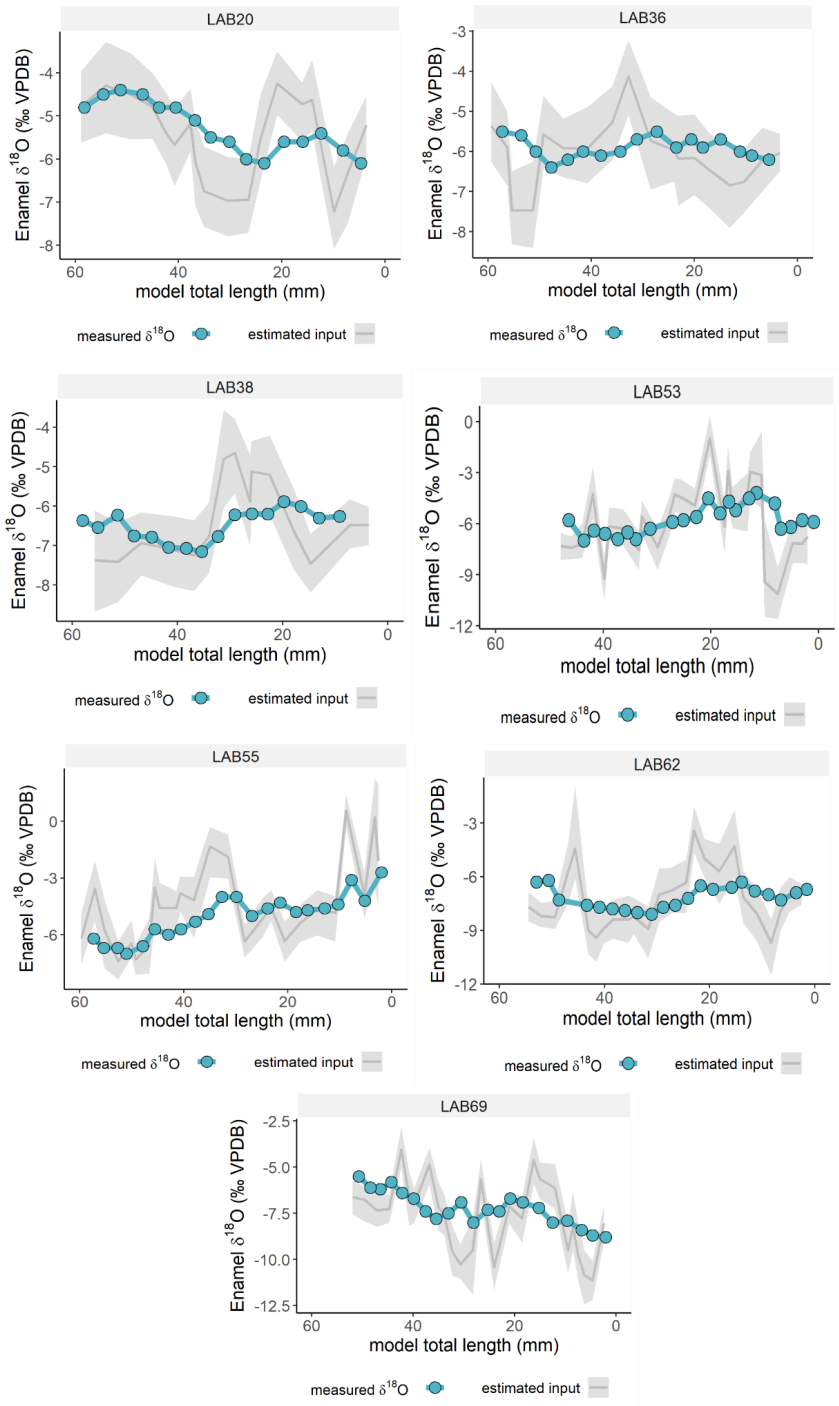

Figure D4. Inverse models for oxygen isotope composition ($\delta^{18}O$) from teeth from Labeko Koba, considering distance from enamel root junction. The blue line and points correspond to original data and grey line the most likely model solution, with the 95% confidence interval shown in shaded areas.

https://doi.org/10.5194/bg-2023-128
Preprint. Discussion started: 9 August 2023
© Author(s) 2023. CC BY 4.0 License.

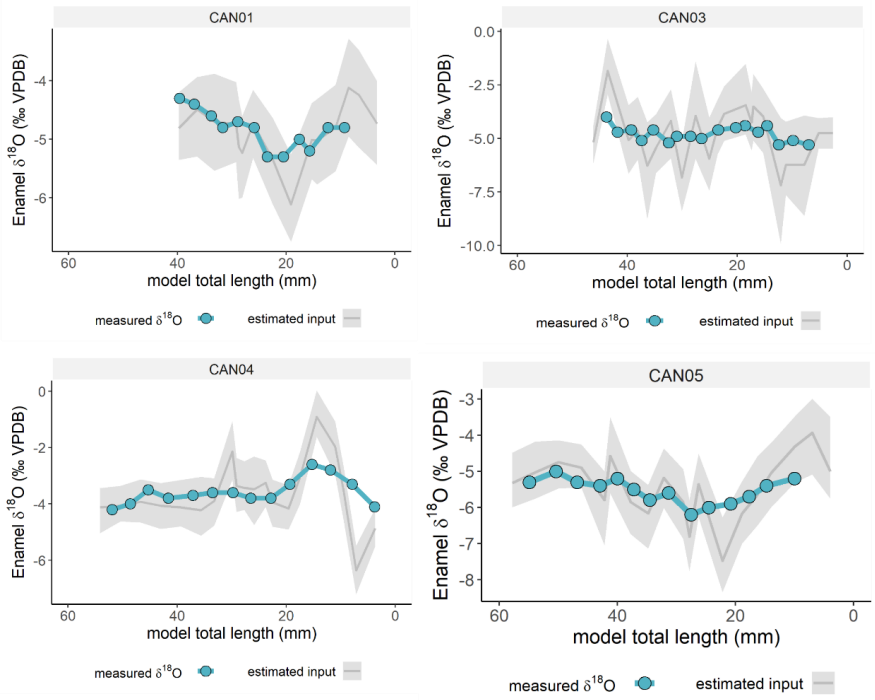

Figure D5. Inverse models for oxygen isotope composition ($\delta^{18}O$) from teeth from Canyars considering distance from enamel root junction. The blue line and points correspond to original data and grey line the most likely model solution, with the 95% confidence interval shown in shaded areas.

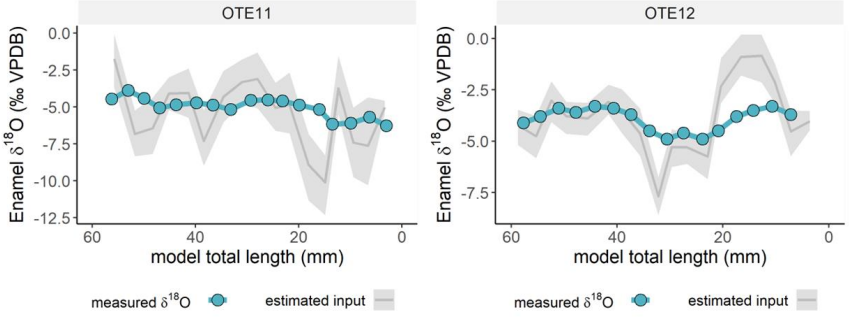

Figure D6. Inverse models for oxygen isotope composition ($\delta^{18}O$) from teeth from El Otero, considering distance from enamel root junction. The blue line and points correspond to original data and grey line the most likely model solution, with the 95% confidence interval shown in shaded areas.

https://doi.org/10.5194/bg-2023-128
Preprint. Discussion started: 9 August 2023
© Author(s) 2023. CC BY 4.0 License.

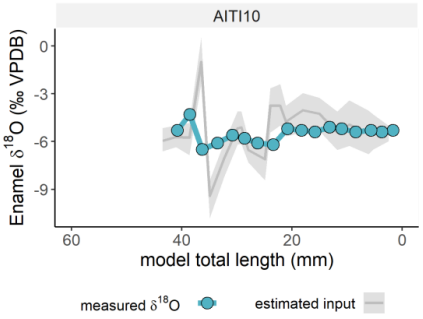

Figure D7. Inverse models for oxygen isotope composition ($\delta^{18}O$) from teeth from Aitzbitarte III, considering distance from enamel root junction. The blue line and points correspond to original data and grey line the most likely model solution, with the 95% confidence interval shown in shaded areas.

References Appendix D

Bendrey, R., Vella, D., Zazzo, A., Balasse, M., Lepetz, S., 2015. Exponentially decreasing tooth growth rate in horse teeth: implications for isotopic analyses. Archaeometry 57, 1104–1124. https://doi.org/10.1111/arcm.12151

Blumenthal, S.A., Cerling, T.E., Chritz, K.L., Bromage, T.G., Kozdon, R., Valley, J.W., 2014. Stable isotope time-series in mammalian teeth: In situ δ18O from the innermost enamel layer. Geochim. Cosmochim. Acta 124, 223–236. https://doi.org/10.1016/j.gca.2013.09.032

Kohn, M.J., 2004. Comment: Tooth Enamel Mineralization in Ungulates: Implications for Recovering a Primary Isotopic Time-Series, by B. H. Passey and T. E. Cerling (2002). Geochim. Cosmochim. Acta 68, 403–405. https://doi.org/10.1016/S0016-7037(03)00443-5

Passey, B.H., Cerling, T.E., 2002. Tooth enamel mineralization in ungulates: implications for recovering a primary isotopic time-series. Geochim. Cosmochim. Acta 66, 3225–3234. https://doi.org/10.1016/S0016-7037(02)00933-X

Passey, B.H., Robinson, T.F., Ayliffe, L.K., Cerling, T.E., Sponheimer, M., Dearing, M.D., Roeder, B.L., Ehleringer, J.R., 2005. Carbon isotope fractionation between diet, breath CO2, and bioapatite in different mammals. J. Archaeol. Sci. 32, 1459–1470. https://doi.org/10.1016/j.jas.2005.03.015

Zazzo, A., Bendrey, R., Vella, D., Moloney, A.P., Monahan, F.J., Schmidt, O., 2012. A refined sampling strategy for intra-tooth stable isotope analysis of mammalian enamel. Geochim. Cosmochim. Acta 84, 1–13. https://doi.org/10.1016/j.gca.2012.01.012